Wang et al. *Zool. Res.* 2025, 46(3): 576−607
https://doi.org/10.24272/j.issn.2095-8137.2024.387
https://cstr.cn/32248.14.zr.2024.387

ZR | Zoological Research

Review Open Access

# Cardiac rehabilitation in porcine models: Advances in therapeutic strategies for ischemic heart disease

Shi-Qi Wang[1,2,#], Ting-Yu Chen[3,#], Lu Wang[1,2,#], Hong-Xin Cheng[1,2], Han-Bin Li[1,2], Cheng-Qi He[1,2], Chen-Ying Fu[4,5,*], Quan Wei[1,2,*]

[1] *Rehabilitation Medicine Center and Institute of Rehabilitation Medicine*, *West China Hospital*, *Sichuan University*, *Chengdu*, *Sichuan* 610041, *China*

[2] *Key Laboratory of Rehabilitation Medicine in Sichuan Province*, *Chengdu*, *Sichuan* 610041, *China*

[3] *Department of Radiology*, *West China Hospital*, *Sichuan University*, *Chengdu*, *Sichuan* 610041, *China*

[4] *State Key Laboratory of Biotherapy and National Clinical Research Center for Geriatrics*, *West China Hospital*, *Sichuan University*, *Chengdu*, *Sichuan* 610041, *China*

[5] *Aging and Geriatric Mechanism Laboratory*, *West China Hospital*, *Sichuan University*, *Chengdu*, *Sichuan* 610041, *China*

## ABSTRACT

Ischemic heart disease (IHD) remains a leading contributor to cardiovascular disease (CVD) worldwide. Despite advances in diagnostic and therapeutic approaches, translational research demands robust large animal models to bridge the gap between experimental interventions and clinical application. Among these, porcine models have gained prominence due to their anatomical, physiological, immunological, and genomic similarities to humans. This review provides a comprehensive overview of current methodologies for establishing porcine IHD models, critically assesses emerging rehabilitative strategies, and outlines innovative therapeutic technologies, with the goal of guiding model selection and fostering the development of novel treatment strategies.

**Keywords:** Ischemic heart disease; Cardiovascular disease; Porcine model; Rehabilitation; Physical therapy modality

## INTRODUCTION

Cardiovascular diseases (CVDs) have emerged as the leading cause of global morbidity and mortality, with ischemic heart disease (IHD) constituting the most prevalent and lethal subtype. Although IHD incidence varies geographically (Zwack et al., 2023), it is defined by myocardial insufficiency, the underlying pathogenesis of which is atherosclerotic obstruction, coronary artery spasm, or microvascular dysfunction (Jensen et al., 2020). Despite its chronic and progressive nature, IHD can acutely deteriorate, often triggered by plaque rupture or erosion, leading to thrombosis and myocardial infarction (MI). The World Health Organization consistently ranks IHD among the top causes of death worldwide, placing a heavy burden on individuals, families, and societies (Han et al., 2020).

Typically, IHD includes a spectrum of clinical manifestations, including acute coronary syndrome and MI, all of which involve structural and functional compromise of blood vessels and cardiac tissue. Although thrombolysis, coronary stenting, revascularization, antiplatelet therapy, and lipid-lowering therapy have significantly reduced mortality, therapeutic strategies that directly restore or regenerate myocardial architecture remain limited (Figure 1) (Eckhouse et al., 2013). In recent years, the domain of cardiac rehabilitation has evolved, incorporating technological advancements to improve cardiopulmonary function and exercise capacity in patients with IHD, although individualized training intensities result in variable prognostic outcomes (Boyne et al., 2023). Notably, researchers in rehabilitation science are increasingly exploring innovative and integrative strategies for IHD treatment, driven by a growing body of preclinical evidence (Feliciano et al., 2022; Wang et al., 2023).

The development and rehabilitation of animal models for IHD continue to present significant challenges (Hou et al., 2022). Integrating advanced or multimodal rehabilitation



Received: 14 February 2025; Accepted: 11 March 2025; Online: 12 March 2025

Foundation items: This work was supported by the National Key R&D Program of China (2023YFC3603800, 2023YFC3603801), National Natural Science Foundation of China (82202793, 82172534, 82372574), Natural Science Foundation of Sichuan Province (2023NSFSC1999, 2023NSFSC1495), Young and Middle-Aged Leading Talent Cultivation Project of Sichuan University (JH20231160), Noncommunicable Chronic Diseases-National Science and Technology Major Project (2024ZD0526000), and 1·3·5 Project for Disciplines of Excellence, West China Hospital, Sichuan University (ZYJC21038)

[#]Authors contributed equally to this work

*Corresponding authors, E-mail: fcying_2004@163.com; weiquan@scu.edu.cn

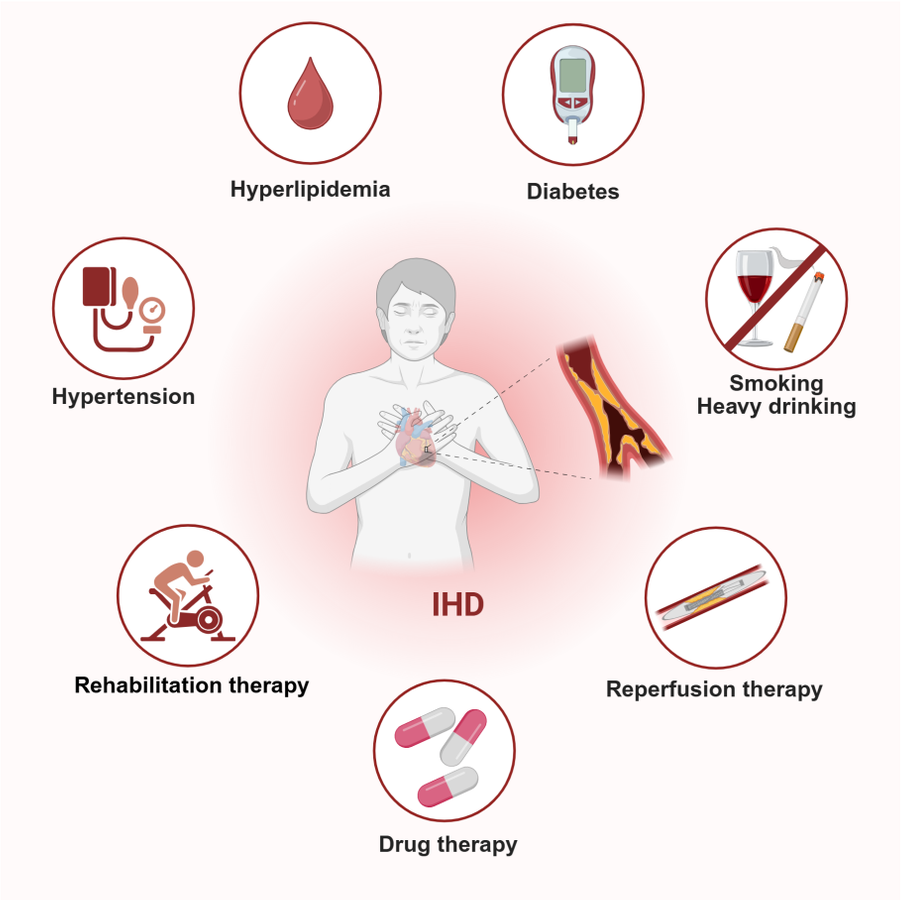


**Figure 1 Prevention and treatment strategies for IHD**

Management of IHD includes risk factor management, medication, and reperfusion therapy to fully control damage caused by disease progression. Illustration was created by BioRender.com. IHD: Ischemic heart disease.

strategies into large animal models is indispensable for bridging preclinical findings with clinical application and remains a cornerstone of translational cardiovascular research (Eun et al., 2017). Although small animal models have been instrumental in elucidating the cellular and molecular mechanisms underlying rehabilitation therapies, their limited anatomical and physiological relevance to the human cardiovascular systems impedes successful clinical translation (Lunney et al., 2021). In contrast, large animal models can more effectively replicate the progression of human heart disease and provide a more realistic and clinically relevant framework for evaluating the efficacy and feasibility of novel rehabilitation interventions.

In cardiac rehabilitation research, large animal models such as pigs, dogs, and sheep have become indispensable due to their physiological and anatomical resemblance to humans, which enables more accurate simulation of human cardiovascular pathology. Among these, porcine models are particularly valuable due to their comparable cardiac anatomy, coronary circulation, immune responses, and genomic architecture (Netzley & Pelled, 2023). These similarities facilitate the creation of clinically relevant models of IHD, such as atherosclerosis (AS) and MI, through surgical procedures, pharmacological induction, and genetic modification, providing a robust experimental platform for evaluating diagnostic approaches and rehabilitation strategies for cardiovascular diseases (Niccoli et al., 2016).

This review presents a comprehensive overview of current methodologies for establishing porcine models of IHD, alongside an in-depth analysis of associated rehabilitation strategies and emerging therapeutic technologies, with the aim to support informed model selection and stimulate the development of clinically translatable treatment strategies. Emphasis is placed on widely adopted models, including AS, MI, ischemia-reperfusion (I/R) injury, and heart failure (HF), and their utility in replicating human pathophysiological conditions. The integration of these models into cardiac rehabilitation research offers a powerful platform for simulating disease progression and therapeutic response, thereby enhancing the relevance and applicability of preclinical findings to human IHD management.

## PIGS AS A PREFERRED LARGE ANIMAL MODEL FOR IHD RESEARCH

Pigs have emerged as an optimal large animal model for IHD research, primarily due to their close anatomical, physiological, and pathophysiological resemblance to humans.

### Similarity in anatomical structure and physiological function

The coronary anatomy of pigs closely mirrors that of humans, with left and right coronary arteries originating from the aortic root and branching into the atrial and ventricular territories. Notably, the porcine heart exhibits minimal coronary collateralization, facilitating the reproducible induction of ischemic injury and making it particularly suitable for MI

models (Jia et al., 2024; Kuwahara et al., 2004; Thirugnanasambandam et al., 2022). Furthermore, contractile dynamics of the pig heart, including rhythmic systole and diastole, replicate human heart cycles with high fidelity, allowing for physiologically relevant simulation of human cardiac responses under disease states. Both heart size and vascular dimensions in adult pigs are highly similar to those in humans, enabling reliable hemodynamic studies, with key parameters, such as resting left ventricular (LV) pressure, heart rate, and cardiac output, closely matching those observed in humans (Li et al., 2024; Sheu et al., 2024). In summary, the anatomical and physiological congruence between porcine and human hearts enhances the translational value of pig models in IHD research. These models not only enable precise replication of human cardiac pathophysiology but also provide a robust framework for exploring the efficacy and safety of various treatment strategies.

**Similarity in disease response**

Pigs exhibit pathophysiological responses to ischemic injury that closely parallel those observed in humans, making them ideal for modeling IHD progression. Interventions such as coronary artery ligation or balloon occlusion reliably induce pathological states such as myocardial ischemia and infarction, replicating the cascade of pathological events characteristic of human disease (Loen et al., 2023; Pei et al., 2024). In addition, the application of gene editing technologies in pigs allows for precise manipulation of disease pathways, enabling the development of chronic IHD models (Hou et al., 2022). Under pathological conditions, pig hearts exhibit various phenotypes, including oxidative stress, cardiomyocyte death, and myocardial fibrosis, thus providing critical insight into disease mechanisms and therapeutic targets (Stevic et al., 2024; Wei et al., 2025).

## ESTABLISHMENT AND EVALUATION OF PORCINE AS MODELS

AS is a multifactorial, lipid-driven, arterial immunoinflammatory disease, with coronary AS representing the most common clinical manifestation of IHD. Multiple risk factors, such as smoking, sex-related hormonal influences, metabolic disturbances, and chronic systemic inflammation, accelerate lipid infiltration into the inner membrane, initiating plaque formation and arterial remodeling (Falk, 2006). Progressive lumen stenosis and endothelial dysfunction impair coronary blood flow, resulting in a mismatch between myocardial oxygen supply and consumption. This cascade leads to sustained myocardial ischemia and hypoxia (Feng et al., 2021), ultimately causing irreversible cardiomyocyte damage, contractile dysfunction, and impaired quality of life. To investigate the etiology, diagnosis, and rehabilitation of AS, porcine models have been successfully established using diverse methodologies, including surgical interventions, dietary or pharmacological induction, and genetic modification. Notably, porcine models recapitulate key pathological and anatomical features of human AS that are poorly represented in small animal models. These include lesion development at anatomically relevant sites, particularly the proximal end of the coronary arteries, foam cell accumulation, neovascularization within plaques, and calcified granule formation (Shim et al., 2016). Such features are critical for studying plaque instability, vascular remodeling, and therapeutic response. This review focuses on the establishment of porcine AS models, with particular emphasis on coronary atherosclerosis (CAS) models, and outlines the techniques used to replicate human disease progression with high fidelity (Figure 2).

**High-fat diet**

Although pigs are inherently susceptible to developing AS with age, even when maintained on standard diets, the natural course of disease progression is typically slow and resource-intensive, thereby increasing the expenses associated with feeding. To accelerate disease onset and improve experimental efficiency, high-cholesterol diets are frequently employed as a reliable strategy for inducing AS in pigs (Simon et al., 2022; Ma et al., 2023b).

The rate and extent of AS development following high-fat feeding are influenced by several factors, including the specific composition of the diet, duration of feeding, breed and age of the pig, and housing conditions. In general, early-stage AS lesions can be observed within weeks to a few months after initiating a cholesterol-enriched diet. Serial collection of blood and vascular tissue during the feeding period enables dynamic monitoring of lesion progression through biochemical indicators and histopathological analysis. While high-fat diet induction is straightforward and cost-effective, it lacks consensus regarding the optimal cholesterol concentration required to induce consistent and clinically relevant AS. Furthermore, consuming substantial cholesterol-rich feed may result in the accumulation of cholesterol across multiple organs. Consequently, most current studies utilize high-fat feed with a cholesterol content not exceeding 2%.

**Balloon compression**

Endothelial disruption and lipid infiltration are central to the pathogenesis of AS lesions. To replicate these initiating events, CAS models can be established by artificially damaging the integrity of the coronary intima to promote the formation of foam cells. Among available techniques, balloon compression injury has become a widely adopted method for modeling coronary artery damage in large animals (Kim et al., 2021). This approach involves the insertion of a balloon catheter into the target blood vessel, followed by controlled inflation and repeated mechanical dilation to simulate vascular injury and early AS processes. However, while balloon compression effectively initiates vascular remodeling and lesion formation, these models typically lack the full pathological complexity of human AS.

**Gene editing**

Gene editing technology has revolutionized the field of disease modeling by enabling precise, targeted modifications at the genomic level, thereby allowing the replication of human disease-associated gene mutations in animal systems. In the context of AS, this technology facilitates the generation of porcine models with specific genetic backgrounds and carrying specific genetic alterations known to disrupt lipid metabolism and promote disease progression. Key targets include apolipoprotein E (ApoE) and the low-density lipoprotein receptor (LDLR), which significantly increase basal plasma cholesterol and accelerate AS formation (Kamato et al., 2022). These genetically modified models can closely recapitulate the chronic progression of human atherosclerotic disease, from MI to HF, providing a more comprehensive representation of the underlying pathophysiological mechanisms. Established gene editing approaches include ApoE-knockout (ApoE-KO), LDLR knockout (LDLR-KO), and

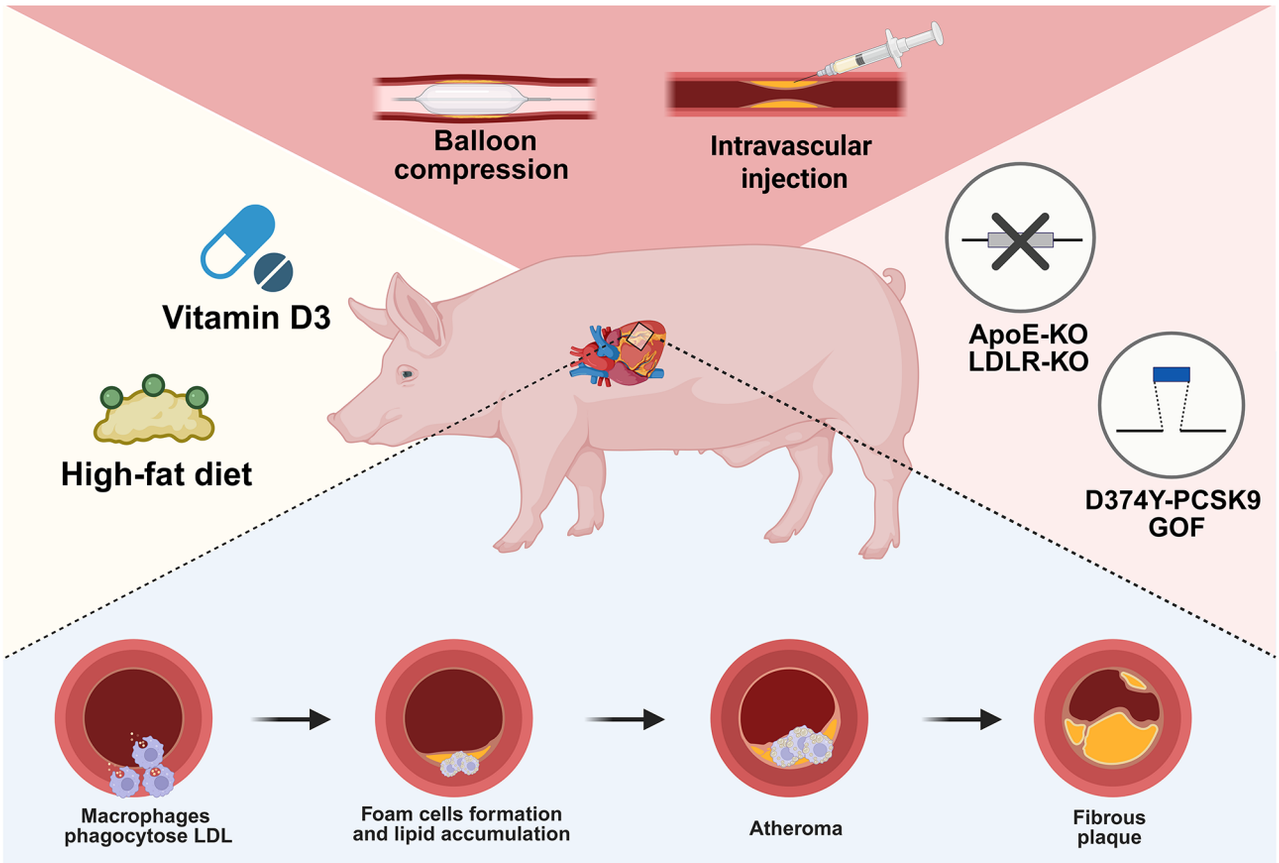


**Figure 2 Establishment of porcine AS model**

AS can be induced by a high-fat diet or endothelial damage. High-fat diet increases LDL in the blood and promotes its oxidation and foam cell formation. Endothelial injury triggers an inflammatory response, which accelerates LDL deposition and plaque development, leading to atherosclerotic lesions. Constructing gene-edited pigs or adding vitamin D3 or bovine serum albumin to a high-fat diet can shorten AS establishment time. Illustration was created by BioRender.com. ApoE: Apolipoprotein E; AS: Atherosclerosis; GOF: Gain-of-function; KO: Knockout; LDL: Low-density lipoprotein; LDLR: Low-density lipoprotein receptor.

D374Y-PCSK9 gain-of-function (GOF) (Wang et al., 2020a).

**ApoE-KO:** ApoE plays a central role in lipoprotein clearance and lipid homeostasis, and its deficiency is strongly associated with human cardiovascular pathology. In genetically modified minipigs, ApoE deficiency increases residual lipoproteins and accelerates progressive AS (Shim et al., 2017). CRISPR/Cas9-generated ApoE$^{-/-}$ pigs exhibit a moderate increase in plasma cholesterol when fed a normal diet but develop severe hypercholesterolemia and spontaneous AS-like lesions in the aorta and coronary arteries when fed a high-fat, high-cholesterol diet for 6 months (Fang et al., 2018). Although ApoE gene disruption significantly increases susceptibility to a high-fat diet, the prohibitive costs and technical challenges associated with achieving gene knockout in pigs have hindered its application in preclinical research (Getz & Reardon, 2022). Nonetheless, ApoE-KO pigs represent a valuable large animal model for testing therapeutic interventions in the context of developing and advanced coronary artery disease.

**LDLR-KO:** Deletion of the LDLR gene can lead to an increase in low-density lipoprotein cholesterol (LDL-C) levels and AS lesion formation. LDLR$^{+/-}$ pigs have been successfully generated using recombinant adeno-associated virus-mediated gene targeting and somatic cell nuclear transfer, with subsequent breeding yielding LDLR$^{-/-}$ pigs. When fed normal low-fat, cholesterol-free feed, LDLR$^{+/-}$ pigs present moderate and persistent increases in total (TC) and LDL cholesterol, whereas LDLR$^{-/-}$ pigs develop severe hypercholesterolemia and AS lesions in the coronary arteries and abdominal aorta similar to those in humans (Davis et al., 2014). LDLR gene knockout can also be achieved by deleting the exonic region from cultured porcine embryonic fibroblasts to establish LDLR$^{-/-}$ pigs (Konishi et al., 2020; Li et al., 2016; Ogita et al., 2016). Combining LDLR deficiency with high-cholesterol diets or balloon-induced endothelial injury produces CAS models with high reproducibility and pathological fidelity (Ogita et al., 2016). Huang et al. (2017) successfully applied CRISPR/Cas9 to Bama miniature pigs to simultaneously target ApoE and LDLR, successfully generating biallelic knockout pigs with elevated levels of LDL-C, TC, and ApoB.

**D374Y-PCSK9 GOF:** D374Y GOF mutation in the proprotein convertase subtilisin 9 (PCSK9) gene can induce severe autosomal dominant hypercholesterolemia and accelerate human AS development (Poulsen et al., 2018). Transgenic pigs expressing human D374Y-PCSK9 specifically in the liver have been generated using *Sleeping Beauty* DNA transposition and somatic cell nuclear transfer (Hamamdzic & Wilensky, 2013). These pigs display markedly reduced hepatic LDLR levels, impaired LDL clearance, severe hypercholesterolemia, and spontaneous progressive atherosclerotic lesions (Al-Mashhadi et al., 2013). Although

the duration of high-fat feeding required to elicit comparable phenotypes may vary among pig breeds, the D374Y-PCSK9 model consistently produces robust hyperlipidemia and lesion development (Yuan et al., 2018). Notably, targeted elevation of renal artery pressure in PCSK9-D374Y pigs has been shown to enhance LDL infiltration into the coronary artery intima, further accelerating CAS formation and offering novel insights into the hemodynamic modulation of atherogenesis (Al-Mashhadi et al., 2021).

**Other methods**

Several alternative approaches have been explored for inducing AS in animal models, including the intravascular administration of lipids or proinflammatory factors to induce localized vascular reactions and eventually AS. However, while these methods can initiate early-stage vascular changes, they cannot fully mimic the characteristics of advanced atherosclerotic plaques in humans and have therefore seen limited adoption in preclinical research (Buszman et al., 2019; Lee et al., 2018). Pharmacological induction strategies have also been investigated, specifically the co-administration of a high-fat diet with agents such as vitamin D3 and bovine serum albumin, which appears to enhance lesion development compared to dietary intervention alone (Lian et al., 2018). Nevertheless, these approaches have not yet been utilized for CAS modeling in larger animals.

**Evaluation of AS models**

Successful model establishment depends on comprehensive evaluation using hematological, imaging, and histopathological assessments. Hematological evaluation primarily involves serum lipid profiling to monitor changes in cholesterol metabolism. High-fat diet administration in pigs typically leads to elevated levels of TC, LDL cholesterol, and high-density lipoprotein (HDL) cholesterol (Grinstead et al., 1994), the latter potentially reflecting a concurrent increase in baseline cholesterol induced by the high-fat diet (Miller et al., 2017). For anatomical and functional assessment of CAS, coronary angiography and intravascular ultrasound are the principal imaging modalities. These techniques allow real-time visualization of arterial morphology and enable quantification of the area of stenosis in the vascular lumen (Choy et al., 2015). Following euthanasia, the anterior descending coronary artery can be rapidly isolated for histological analysis by Oil Red O and hematoxylin-eosin (H&E) staining (Emini Veseli et al., 2017).

## ESTABLISHMENT AND EVALUATION OF PORCINE MI AND I/R INJURY MODELS

MI represents one of the most severe forms of IHD, primarily resulting from thrombotic occlusion triggered by plaque rupture, erosion, or coronary vasospasm. At the cellular level, MI induces a cascade of pathological events, including a shift to anaerobic metabolism, rapid depletion of energy storage, loss of membrane integrity, disruption of ionic gradients, impaired contractility, and heightened susceptibility to arrhythmias (Gill, 1991). While reperfusion therapy remains the standard clinical treatment, its abrupt restoration of blood flow can lead to I/R injury, characterized by the accumulation of calcium ions and generation of free radicals (Algoet et al., 2023). As such, the development of effective rehabilitation strategies targeting both MI and I/R injury is a major focus in translational research utilizing porcine models.

Surgical induction of MI in pigs enables controlled simulation of human disease processes. Two principal model types are commonly used: permanent closure and I/R injury. These models differ based on whether coronary blood flow is restored following arterial blockage. Permanent occlusion models are used to replicate the pathophysiological conditions observed in patients who have not received coronary stenting due to contraindications or treatment delays. In contrast, I/R injury models simulate the pathophysiological alterations occurring in tissues of patients undergoing reperfusion therapy following the restoration of blood flow interruption (Lou et al., 2023; Patel et al., 2023). Both approaches enable the investigation of distinct mechanisms of myocardial injury and recovery and can be established using two widely accepted surgical techniques (Figure 3).

**Coronary artery ligation**

Thoracotomy-based coronary artery ligation remains a widely used technique for inducing MI in porcine models. The procedure involves administering anesthesia and endotracheal intubation, followed by assisted ventilation. After a thoracic incision, the chest wall is carefully dissected to locate and ligate the coronary artery. The specific ligation site may vary depending on the experimental objectives, with the left anterior descending branch and left circumflex branch commonly targeted in most studies (Avendaño et al., 2023; Liao et al., 2021). For I/R injury models, vascular recanalization is accomplished by releasing the silk thread after a designated duration of coronary artery ligation. Preoperative isolation of the artery and vein, along with preischemic conditioning, has been shown to enhance model reproducibility and survival rates (Zhou et al., 2023).

However, this method carries notable risks. Permanent ligation is associated with a high incidence of fatal arrhythmias, such as ventricular fibrillation and ventricular tachycardia, which may lead to collateral vessel growth and poor modeling efficacy (Einstein & Abdul-Hussein, 1995). In addition, different ischemia durations in I/R injury models can influence the incidence of malignant arrhythmias, underscoring the need to explore successful model establishment based on laboratory settings, operator expertise, and study objectives.

Despite being invasive and associated with an elevated risk of postoperative infection, thoracotomy enables direct assessment of myocardial morphology and coronary blood flow. Due to its technical accessibility, cost-effectiveness, and capacity for controlled infarct induction, coronary artery ligation remains a common technique for preclinical MI and I/R research in pigs.

**Interventional surgery for coronary artery occlusion**

Advances in interventional cardiology have facilitated the development of minimally invasive methods to induce MI in porcine models by occluding coronary arteries using autologous thrombi, gelatin sponges, or balloons (Jiang et al., 2023; Schüttler et al., 2022). These procedures mirror clinical interventional practices, whereby catheters are introduced through the right femoral artery or common carotid artery to occlude or recanalize the distal end of the heart. In gelatin sponge embolization, a gelatin matrix is delivered via a contrast catheter following coronary angiography to achieve permanent occlusion, typically used to establish a stable MI model without subsequent reperfusion (Sun et al., 2018). Conversely, balloon occlusion offers greater flexibility for I/R

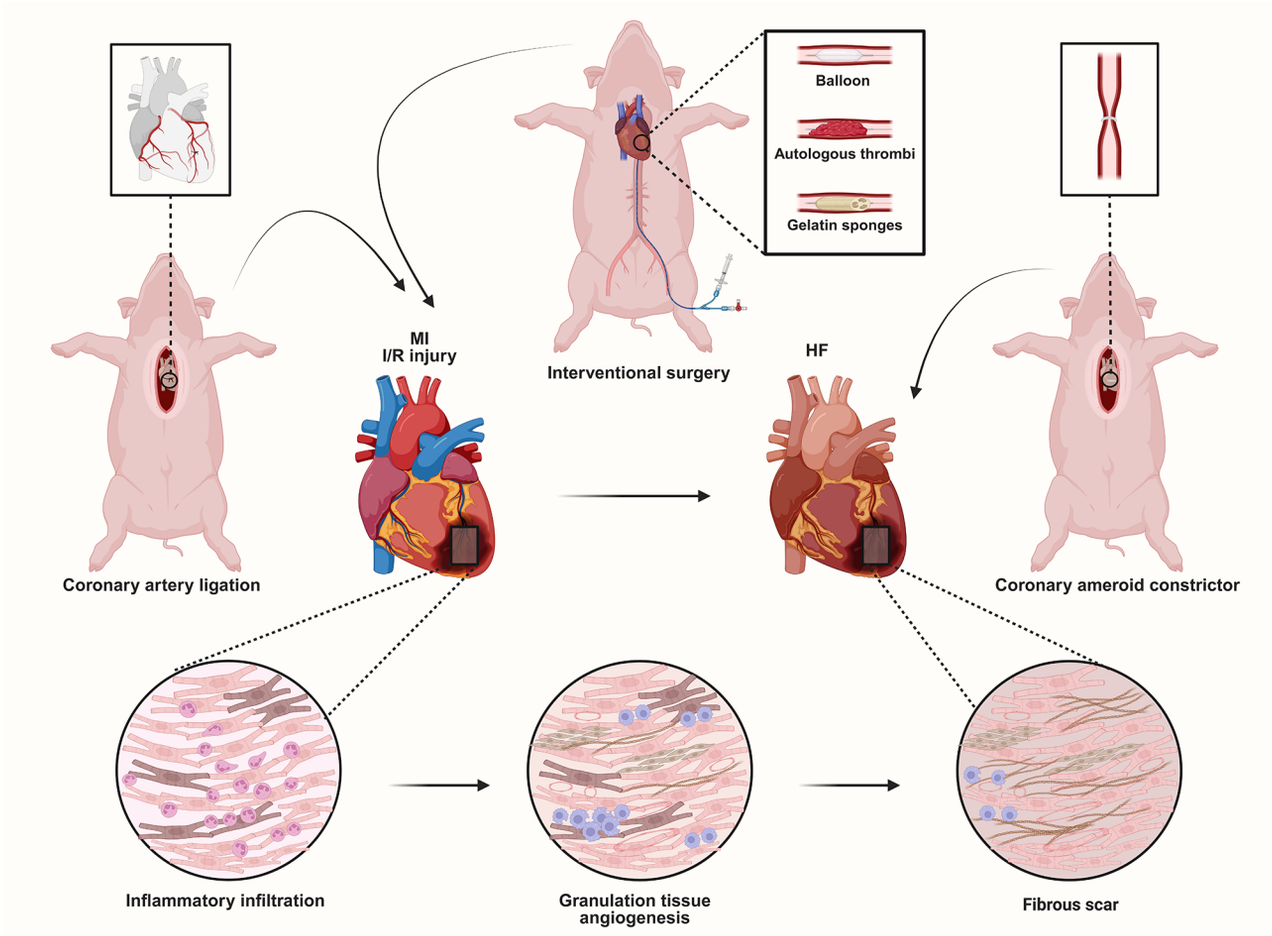


**Figure 3 Establishment of porcine MI, I/R injury, and HF models**

Permanent MI and I/R injury models can be established by coronary artery ligation via thoracotomy or interventional surgery to block the target coronary artery. Myocardial ischemia and hypoxia occur after coronary artery occlusion. Inflammatory cells rapidly infiltrate damaged myocardium to remove necrotic tissue. Granulation tissue subsequently forms, but excessive repair results in the progressive replacement of the myocardium by fibrotic tissue. As the disease progresses, the pumping function of the heart becomes severely impaired, leading to HF. An HF model can also be established by an ameroid constrictor, leading to chronic ischemia of coronary arteries. A hygroscopic ameroid constrictor ring is surgically placed around a coronary artery in pigs, where it gradually swells, causing chronic ischemia, myocardial dysfunction, and HF. Cardiac function is monitored via echocardiography and hemodynamic assessment, validating the model for ischemic HF research. Illustration was created by BioRender.com. HF: Heart failure; I/R: Ischemia-reperfusion; MI: Myocardial infarction.

models by allowing temporary vascular occlusion and subsequent reopening (Brenner et al., 2021; Silvis et al., 2022). Additionally, some studies have employed percutaneous deployment of permanent coils into the proximal marginal branches or circumflex artery branches to induce left lateral MI (Adeliño et al., 2022; Martínez-Falguera et al., 2021); however, this method has not yet been applied on a large scale.

Compared with traditional thoracotomy ligation, interventional approaches offer several advantages, including reduced invasiveness, absence of tracheal intubation, and lower rates of postoperative infection. These factors collectively contribute to shorter recovery times, higher procedural efficiency, and improved animal welfare (Sakaguchi et al., 2003). Moreover, fluoroscopic guidance enhances the precision of coronary artery targeting, enabling more consistent and reproducible occlusion.

Despite these advantages, interventional occlusion demands a high level of technical expertise in catheter manipulation and places stringent requirements on laboratory facilities and imaging equipment. Procedural success and model stability are highly sensitive to variables such as balloon positioning, inflation pressure, and the hemodynamic state of the animal. Overinflation of the balloon may lead to serious complications such as coronary artery dissection, intima tearing, thrombosis, and exacerbated myocardial injury, underscoring the need for meticulous procedural control.

### Evaluation of MI and I/R injury models

Successful model establishment depends on a comprehensive evaluation integrating physiological, imaging, hematological, hemodynamic, and pathological assessments (Chen et al., 2013; Sun et al., 2020; Yang et al., 2023). Intraoperative and early postoperative monitoring of physiological indicators is essential, with the appearance of ST-segment elevation on electrocardiography serving as a primary indicator of effective coronary artery ligation or occlusion. In addition, imaging techniques, such as echocardiography, are routinely employed to assess cardiac function after MI, revealing characteristic reductions in ventricular wall motion and altered septal and apical dynamics following infarction. Likewise,

cardiac magnetic resonance (CMR) imaging offers a more detailed evaluation, enabling early detection of myocardial edema and necrosis. In later stages, CMR provides accurate quantification of infarct size and scar tissue development, critical for assessing long-term outcomes.

Current hematological evaluation focuses on the detection of postoperative MI biomarkers, such as troponin, creatine kinase isoenzyme, and myoglobin (Duan et al., 2015), which peak shortly after infarction but decline over time, necessitating prompt sample collection. Histopathological analysis following euthanasia remains a gold standard for definitive assessment. Techniques such as 2,3,5-triphenyltetrazolium chloride (TTC) staining for infarct delineation, along with Sirius Red, Masson trichrome, and hematoxylin-eosin (H&E) staining, enable detailed characterization of infarct extent, fibrotic remodeling, and myocardial architecture (Yang et al., 2022b).

## ESTABLISHMENT AND EVALUATION OF PORCINE HF MODELS

HF is a complex clinical syndrome and a common manifestation of advanced IHD, often occurring in the terminal stages of disease progression (Völz et al., 2021). Coronary artery disease is recognized as a major risk factor for the development of HF, and persistent myocardial ischemia frequently contributes to its development by inducing structural and functional alterations within the coronary circulation (Pagliaro et al., 2020). Based on cardiac function, HF is typically classified into two major phenotypes: HF with preserved ejection fraction (HFpEF) and HF with reduced ejection fraction (HFrEF).

The pathogenesis of HF involves progressive ventricular remodeling, driven by abnormal load conditions, neurohormonal activation, genetic predisposition, and concomitant comorbidities. These factors can alter the size, shape, and functional capacity of the failing heart. Remodeling patterns determine the rearrangement of cardiomyocytes, fibrocytes, and blood vessels, ultimately resulting in either ventricular wall stiffness or reduced contractility (Heusch et al., 2014). In HFrEF, ventricular enlargement, transformation in spherical volume, and wall thinning are characteristic structural changes. In contrast, HFpEF is characterized by centripetal remodeling, preservation of ejection fraction, normal or reduced ventricular volume, and increased LV mass-to-volume ratio due to wall thickening (Pagliaro et al., 2020). HFpEF models typically involve an increased afterload of the cardiovascular system, primarily by aortic coarctation, stent implantation, renal hypertension, or induction of mineralocorticoid-driven hypertension. The pathophysiological mechanisms underlying HF differ substantially between HFpEF and HFrEF and have been extensively reviewed (Miyagi et al., 2022).

Successful establishment of porcine HF models is critical not only for studying disease pathogenesis and improving diagnostic accuracy but also for evaluating the impact of emerging rehabilitation strategies on cardiac function and long-term prognosis following HF. Various approaches have been developed to induce HF, all fundamentally based on increasing pre- and postcardiac loads to impair ventricular function (Figure 3). Importantly, modeling approaches must be tailored according to the HF phenotype and specific scientific objectives (Miyagi et al., 2022; Qin et al., 2023). This section summarizes the methods used to establish porcine models of HF secondary to IHD.

### Coronary artery ligation and interventional surgery

Myocardial ischemia and subsequent LV remodeling are primary drivers of HF, making MI models a widely used platform for inducing HF over time. Following the establishment of MI, cardiac function can be regularly monitored via echocardiography, with a decline in ejection fraction typically observed. In porcine models, overt signs of HF generally emerge approximately 4 weeks after MI induction, although the exact timeline depends on multiple factors, including the severity of vessel occlusion, presence of coronary branch blockage, and overall health status of the animal. In addition, a clinically relevant and stable porcine model of decompensated acute heart failure (ADHF) has been developed via occlusion of the circumflex coronary artery 2 weeks after ligation of the left anterior descending coronary artery (Olivari et al., 2022).

### Coronary ameroid constrictors

Ameroid constrictors, typically fabricated from stainless steel or other biocompatible materials, possess an internal structure designed to partially or completely obstruct coronary blood flow. Balloon-based constrictors have also been used to achieve similar effects (Lu et al., 2008). Following thoracotomy under anesthesia, the anterior branch of the left coronary artery, typically located between the left atrial appendage and pulmonary artery, is exposed. An ameroid constrictor is then placed around the artery, with the opening oriented toward the pericardium to facilitate uniform constriction (Xin et al., 2011). Over approximately 3 weeks, progressive occlusion of the coronary artery occurs, resulting in variable degrees of coronary stenosis. This technique offers precise control over the occlusion process, ensures high model stability, and reduces procedural risk compared with direct coronary ligation. By effectively diminishing the extent of myocardial necrosis, the ameroid constrictor model more accurately resembles the pathological features of chronic myocardial ischemia observed in patients with coronary heart disease (CHD).

### Other methods

Induction of atrial fibrillation has also been utilized to model HF. Implantation of a single-chamber atrial pacemaker in pigs can lead to cellular hypertrophy and fibrosis of the atrium and ventricle. This model is beneficial for investigating the pathophysiological mechanisms of atrial fibrillation-associated HF, as well as evaluating therapeutic interventions and rehabilitation strategies (Bauer et al., 2004). In addition, HF can be induced through dietary manipulation; prolonged high-fat feeding promotes coronary atherosclerosis and myocardial dysfunction, closely recapitulating the natural progression of clinical IHD. However, diet-induced models are less controllable in terms of stenosis severity and time to HF onset and may introduce confounding systemic metabolic disorders with long-term feeding.

### Evaluation of HF models

MI and HF models are closely interconnected, with HF frequently representing the terminal stage of MI. Consequently, the evaluation strategies for HF models largely parallel those used for MI models, relying primarily on imaging and histopathological analyses. Echocardiography remains a commonly used and valuable tool for assessing cardiac function, with ejection fraction serving as the principal clinical

and experimental indicator of HF severity. Advanced imaging modalities, such as CMR combined with dedicated image processing tools, allow for detailed visualization and quantification of myocardial perfusion defects, abnormal ventricular wall motion, and degree of myocardial fibrosis, providing a comprehensive evaluation of model success. In addition, histopathological assessments using wheat germ agglutinin (WGA), Sirius Red, and Masson's trichrome staining techniques enable the measurement of myocardial hypertrophy and severity of fibrosis (Li et al., 2022).

## APPLICATIONS OF REHABILITATION IN PORCINE IHD MODELS

### Rehabilitation in AS models

The primary clinical approach to managing coronary atherosclerotic heart disease is secondary prevention, with pharmacological interventions targeting the regulation of blood pressure, glycemic control, and lipid profiles. In parallel, rehabilitation medicine emphasizes structured exercise training to enhance vascular function, cardiorespiratory performance, and overall endurance. The use of porcine models of AS in preclinical rehabilitation research offers an essential platform to refine rehabilitation protocols, ensuring both the safety and efficacy of exercise interventions. These models enable precise evaluation of rehabilitation indications, optimal intervention timing, mechanistic pathways, and therapeutic outcomes, thereby informing clinical translation. At present, most preclinical rehabilitation studies using porcine models have focused on the effects of exercise training in CHD (Figure 4A). Given that endothelial dysfunction is a significant pathological process in coronary atherosclerotic

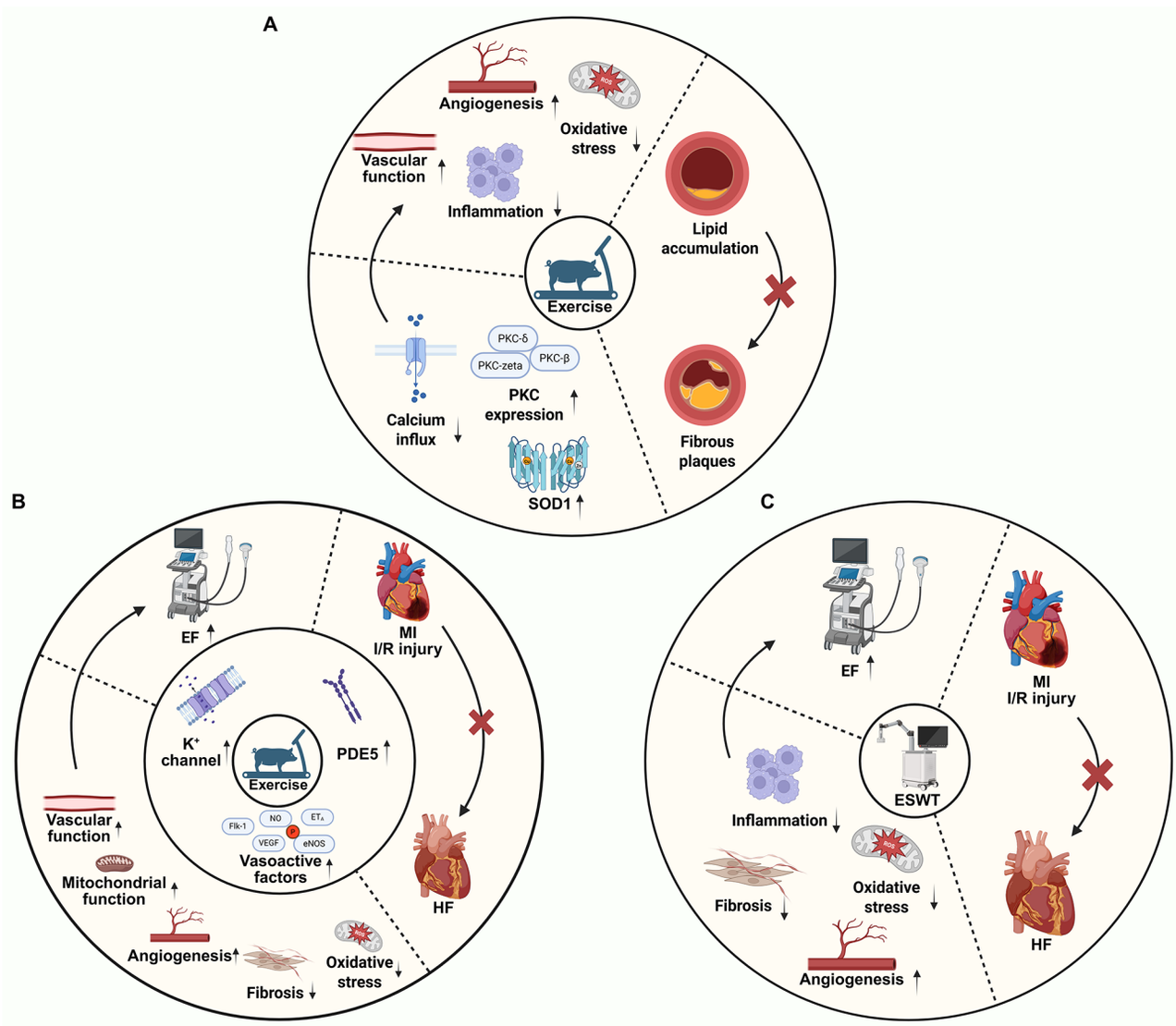


**Figure 4 Pathophysiological changes in porcine IHD models after application of cardiac rehabilitation**

A: Exercise training for porcine AS. Exercise training can regulate coronary vessels and improve inflammation and oxidative stress by regulating ion channels and expression of oxidative stress proteins, thus reducing formation of atherosclerotic plaques. B: Exercise training for porcine MI. Exercise training can regulate coronary artery blood vessels, improve inflammation and oxidative stress, reduce mitochondrial dysfunction, promote angiogenesis, and reduce fibrosis by regulating expression of ion channels and vasoactive factors to improve cardiac function and delay disease progression. C: ESWT for porcine MI. ESWT can improve cardiac function after MI by reducing inflammation, promoting angiogenesis, improving fibrosis, and reducing oxidative stress. Therapeutic mechanisms are summarized from studies based on porcine IHD models and do not cover all therapeutic mechanisms of rehabilitation modalities. Illustration was created by BioRender.com. AS: Atherosclerosis; EF: Ejection fraction; ESWT: Extracorporeal shock wave therapy; HF: Heart failure; IHD: Ischemic heart disease; I/R: Ischemia-reperfusion; MI: Myocardial infarction.

heart disease, physical training has been shown to ameliorate this impairment and facilitate cardiac recovery (Table 1).

Extensive evidence supports the role of exercise training in preventing coronary artery dysfunction (Elagizi et al., 2020; Richardson et al., 2009). In a seminal study, Henderson et al. (2004) showed that a high-fat, high-cholesterol diet significantly impaired endothelium-dependent relaxation in Yucatan miniature pigs during early IHD progression, and that exercise training mitigated or reversed these deleterious effects. However, subsequent research has indicated that the protective impact of exercise on coronary smooth muscle function can be attenuated by a concurrent high-fat diet (Bender et al., 2016; Yang et al., 2007). These findings suggest that exercise training and rational diet control should be regarded as equally important interventions and highlight the need for further research on the interplay between exercise intensity and diet composition to optimize clinical exercise prescriptions for CHD patients.

Porcine AS models also offer critical insights into the molecular mechanisms underlying exercise-mediated vascular protection. Exercise training has been shown to reduce calcium influx linked to CAS (Edwards et al., 2010) and enhance the expression of antioxidant proteins within the coronary vasculature. Notably, although exercise does not induce the transformation of coronary vascular cells from a proatherosclerotic to antiatherosclerotic state, it up-regulates critical antioxidant defenses, such as superoxide dismutase 1 (SOD1), thereby counteracting the oxidative stress induced by hypercholesterolemia (Arce-Esquivel et al., 2012; Simmons et al., 2014). Interestingly, the efficacy of exercise in combating coronary atherosclerotic heart disease may exhibit sex-specific differences due to distinct underlying mechanisms. For instance, exercise induces PKC-β, PKC-δ, and PKC-zeta protein levels in the right coronary artery of male pigs fed a high-fat diet but only increases PKC-δ protein levels in female pigs (Korzick et al., 2005).

Despite its broad benefits, exercise training may not uniformly ameliorate all forms of coronary pathology. In pigs with familial hypercholesterolemia, exercise training attenuates the maximum systolic response of the left circumflex branch to the potent endogenous contractile agent endothelin-1 (ET-1) (Bunker & Laughlin, 2010). However, endurance exercise training has been shown to fail at preventing CAS in patients with familial hypercholesterolemia, providing novel insights into the rehabilitation of patients with genetically related cardiovascular dysfunction (Tharp et al., 2019).

**Rehabilitation in MI, I/R injury, and HF models**

Porcine models of MI, I/R injury, and HF are indispensable platforms for rehabilitation research, particularly for evaluating the therapeutic effects of exercise and physical therapies in IHD. These models also enable the assessment of specific pharmacological interventions during rehabilitation, offering valuable insights into the complex interplay between exercise, medication use, and cardiovascular recovery.

**Exercise:** Following MI, LVEF declines, initiating pathological remodeling that progresses if untreated. Exercise training is widely employed in rehabilitation therapy, with numerous studies utilizing porcine MI, I/R injury, and HF models to explore its effectiveness and associated mechanisms (Table 2). These studies provide compelling evidence for the

**Table 1 Applications of porcine high-fat diet-induced AS models in exercise training**

| Exerciseprescription | Model (AS) | Finding | Limitation | Reference |
|---|---|---|---|---|
| Treadmill running<br>2.5–8 mph<br>5 days/week×16 weeks | High-fat diet | Prevents or reverses effects of a high-fat, high-cholesterol diet on endothelium-dependent dilation of coronary arteries. | Changes in eNOS protein content are not enough to exert physiological effects. | Henderson et al., 2004 |
| Treadmill running<br>2–5 mph<br>5 days/week×16 weeks | High-fat diet | Increases PKC-β, PKC-δ, and PKC-zeta protein levels in male pigs; Increases PKC-δ protein levels in female pigs. | Multiple factors such as sex and species can lead to different results. | Korzick et al., 2005 |
| Treadmill running<br>2–5 mph<br>5 days/week×16–20 weeks | High-fat diet | High-fat diet counteracts beneficial effects of exercise on coronary smooth muscle. | Sex differences in HF differentially place males at risk. | Yang et al., 2007 |
| Treadmill running<br>75% of maximal heart rate<br>4 days/week×14 weeks | High-fat diet | Prevents coronary artery dysfunction. | Exact mechanisms by which diabetic dyslipidemia and exercise alter protein association with LDL are not yet understood. | Richardson et al., 2009 |
| Treadmill running<br>4–8 mph<br>5 days/week×16–20 weeks | High-fat diet | Reduces maximum contractile response of left circumflex to endogenous contractile agent ET-1. | Exact mechanism by which exercise training modifies epicardial adipose tissue is not clear. | Bunker & Laughlin, 2010 |
| Treadmill running<br>2.2–4.8 mph×7–8 weeks | High-fat diet | Reduces storage $Ca^{2+}$ entry associated with coronary AS | Benefit of exercise on skeletal muscle metabolism not seen in *Ossabaw* miniature swine. | Edwards et al., 2010 |
| Treadmill running<br>4–7 mph<br>5 days/week×16–20 week, | High-fat diet | Increases antioxidant protein in coronary arteries. | Results do not support exercise signaling expression of anti-atherogenic endothelial cell phenotype in coronary conduit arteries and arterioles in this model of early-stage CAD. | Arce-Esquivel et al., 2012 |
| Treadmill running<br>2–7 mph<br>5 days/week×16–20 week | High-fat diet | Eliminates adverse effect of hypercholesterolemia on SOD1 expression in thoracic veins. | Initial atherogenic arterial endothelial cell phenotype is lacking. | Simmons et al., 2014 |
| Treadmill<br>1–3 mph | High-fat diet | Severe familial hypercholesterolemia impairs regulation of coronary blood flow and oxygen supply during exercise. | Relationship between plaque burden and coronary arteriovenous $H^+$ concentration gradient is not viewed as cause-and-effect. | Bender et al., 2016 |
| Treadmill running<br>5 days/week×10 week | High-fat diet | Cannot limit coronary AS in pigs with familial hypercholesterolemia. | Influences of testosterone in males and whether similar effects are observed in females is unknown. | Tharp et al., 2019 |

AS: Atherosclerosis; CAD: Coronary artery disease; HF: Heart failure; LDL: Low-density lipoprotein; mph: Miles per hour.

**Table 2 Applications of porcine MI, I/R injury, and HF models in rehabilitation treatment**

| Rehabilitation treatment | Treatment prescription | Model | | Finding | Limitation | Reference |
|---|---|---|---|---|---|---|
| Exercise training | Treadmill 4–stage exercise protocol (1, 2, 3, and 4 km/h) | MI | Coronary artery ligation | Positive inotropic effect of $Ca^{2+}$ sensitizer EMD 57033 did not decrease during exercise post-MI. | Exercise in presence of EMD 57033 results in slightly lower heart rates, whereas pimobendan results in higher heart rates compared to control exercise. | Duncker et al., 2001 |
| | Treadmill 1–4 km/h | MI | Coronary artery ligation | Abnormal perfusion during exercise does not lead to early LV dysfunction post-MI. | Lack of overt anaerobic metabolism even during heavy exercise suggests that myocardial perfusion abnormalities within surviving myocardium do not contribute to cardiac dysfunction in the first few weeks after infarction. | Haitsma et al., 2001 |
| | Treadmill 1–4 km/h | MI | Coronary artery ligation | Effect of NO derived from endothelial NO synthase on regulation of vascular tension during exercise is maintained. | Perturbations in calcium homeostasis of endothelial cells may contribute to selective impairment of ATP-induced vasodilation in swine with MI. | Haitsma et al., 2002 |
| | Treadmill 1–4 km/h | MI | Coronary artery ligation | Increases sympathetic drive and decreased myocardial and coronary beta-adrenergic reactivity during exercise. | Relatively young age of pigs may influence responses of autonomic control mechanisms to MI and subsequent left ventricle remodeling. | Duncker et al., 2005 |
| | Treadmill 1–4 km/h | MI | Coronary artery ligation | During exercise, myocardial $O_2$ supply and consumption of remodeled muscle remain closely matched. | Net contribution of adenosine to regulation of coronary resistance vessel tone is not increased in remodeled myocardium. | Merkus et al., 2005 |
| | Treadmill 0–4 km/h | MI | Coronary artery ligation | Improves pulmonary hypertension after MI. | Increased sensitivity of pulmonary vasculature to exercise as observed in swine model cannot be explained by loss of NO-mediated inhibition of exercise-induced vasoconstriction. | Merkus et al., 2007 |
| | – | MI | Coronary artery ligation | Retention of cMyBP-C phosphorylation helps maintain appropriate dilation during exercise. | Absence of a difference in baseline phosphorylation of PKA target proteins between MI and sham hearts may be related to differences in catecholamine levels. | Boontje et al., 2011 |
| | Treadmill running 1–4 km/h×1–3 weeks | MI | Coronary artery ligation | Nω-nitro-L-arginine enhances vasodilatory effect of tezosentan during exercise in MI pigs. | Specifically designed experiments are needed to discern changes in action of individual COX end products after MI. | de Beer et al., 2011 |
| | Treadmill running heart rates: 210–220 beats/min 30–50 min/day×24–26 days | HF | Ameroid constrictor | Improves myocardial function and coronary collateral reserve of collateral-dependent myocardium. | Coronary collateral circulation is less developed in sedentary pigs than in exercised pigs before protocols commence. | Roth et al., 1990 |
| | Treadmill running 2.5–6 mph 5 days/week×16 weeks | HF | Ameroid constrictor | Improves endothelium-mediated diastole of isolated arteries after coronary artery occlusion. | Differences in effects of exercise training in arteries isolated from coronary-occluded hearts and those from normal nonoccluded hearts are unclear. | Griffin et al., 1999 |
| | Treadmill running 3–5 mph×16 weeks | HF | Ameroid constrictor | Restores adenosine-induced relaxation in chronic occluded distal coronary arteries. | Reason for raining-enhanced sensitivity to adenosine is unknown. | Heaps et al., 2000b |
| | Treadmill running 2.5–6 mph×16 weeks | HF | Ameroid constrictor | Enhances bradykinin-mediated relaxation of left circumflex arteriole, influences ecNOS mRNA expression, and increases NO. | Individual contributions of infarction are unknown. | Griffin et al., 2001 |
| | Treadmill running 3–5 mph×16 weeks | HF | Ameroid constrictor | Differences in t(1/2) myoplasmic free $Ca^{2+}$ accumulation between left circumflex and left anterior descending cells cannot prevented by exercise. | Cause of decreased sarcoplasmic reticulum $Ca^{2+}$ uptake is unknown. | Heaps et al., 2001 |
| | Treadmill running 3–6 mph×16 weeks | HF | Ameroid constrictor | Cannot alter sarcoplasmic reticulum $Ca^{2+}$ offloading in right coronary cells. | Interpretation does not exclude possibility that differences in plasmalemmal $Ca^{2+}$ influx and other Ca-handling mechanisms may be involved. | Jones et al., 2001 |
| | Treadmill running 3–5 mph 5 days/week×12 weeks | HF | Ameroid constrictor | Increases basal tension of distal arterioles in coronary artery occlusion. | Intricate relationships of numerous mechanisms that control coronary vasomotor tone make *in vivo* measures difficult to interpret. | Heaps et al., 2006 |
| | Treadmill running 2–6 mph 5 days/week×12 weeks | HF | Ameroid constrictor | Up-regulates HSP70 and antioxidant enzymes in porcine skeletal muscle. | Mechanisms underlying skeletal muscle dysfunction with heart disease and heart failure remain poorly understood. | Lawler et al., 2006 |

Continued

| Rehabilitation treatment | Treatment prescription | Model | | Finding | Limitation | Reference |
|---|---|---|---|---|---|---|
| | Treadmill running 2–6 mph 5 days/week×16 weeks | HF | Ameroid constrictor | Exercise training and coronary artery occlusion independently stimulate myocardial hypertrophy and induce different gene expression patterns. | Swine of both sexes are used but not evenly balanced across groups. | Boluyt et al., 2007 |
| | Treadmill running 2–6 mph 5 days/week×12 weeks | HF | Ameroid constrictor | $H_2O_2$, in addition to NO, contributes significantly to exercise-induced restoration of endothelium-dependent dilation of coronary arterioles distal to occlusion. | Inability to quantify produced $H_2O_2$ due to current technology limitations, yet allows possible quantitative measurement of $H_2O_2$ in intact arteriolar wall. | Thengchaisri et al., 2007 |
| | Treadmill running 2–6 mph 5 days/week×14 weeks | HF | Ameroid constrictor | Neuropilin-1 plays an important role in exercise-enhanced collateral-dependent coronary vasodilation. | Other vasodilatory pathways, such as endothelial-derived hyperpolarization factors, may also contribute to vasodilatation. | Fogarty et al., 2009 |
| | Treadmill running 3–5 mph 5 days/week×14 weeks | HF | Ameroid constrictor | Increases total eNOS and eNOS phosphorylation levels in collateral-dependent arteries. | Temperature of measuring endothelial cell free $Ca^{2+}$ using fura 2 is different from previous studies. | Zhou et al., 2010 |
| | Treadmill running 3–5 mph 5 days/week×14 weeks | HF | Ameroid constrictor | $Ca^{2+}$ sensitization to cardiac muscle fibrin helps exercise training enhance myocardial function. | Whether findings contribute to increased force generation observed in the model remains undetermined. | Sarin et al., 2011 |
| | Treadmill running 2–5 mph 5 days/week×14 weeks | HF | Ameroid constrictor | Superoxide/$H_2O_2$ pathway helps exercise training enhance endothelium-mediated branch-dependent coronary artery dilation. | Specificity of diethyldithiocarbamate is equivocal. | Xie et al., 2012 |
| | Treadmill running 2–6 mph 5 days/week×14 weeks | HF | Ameroid constrictor | Enhances diastolic effects of nitric oxide, prostaglandin, and large conductance $Ca^{2+}$-dependent $K^+$ channels on nonocclusive and collateral dependent arteries. | Limitations exist regarding contribution of these molecules to overall relaxation response. | Deer & Heaps, 2013 |
| | Treadmill running 4–6 mph 5 days/week×16 weeks | HF | Ameroid constrictor | Induces adaptation of sustained endothelium-dependent coronary artery relaxation mediators. | Role of prostanoids is limited to experiments of sustained bradykinin-mediated relaxation in arteries of nonoccluded pigs. | Heaps et al., 2014 |
| | Treadmill running 4–6 mph 5 days/week×14 weeks | HF | Ameroid constrictor | Enhances function of $ET_{A.}$ | Acute coronary injury models produce adaptations that will potentially change over time. | Robles & Heaps, 2015 |
| | Treadmill running 2–6 mph 5 days/week×14 weeks | HF | Ameroid constrictor | Up-regulates coronary PDE5. | Insufficient samples to measure proteins in coronary arterioles from the four groups. | Zheng et al., 2015 |
| | Treadmill running 3–5 mph 5 days/week×14 weeks | HF | Ameroid constrictor | Enhances KCL-mediated contractility and $Ca^{2+}$ sensitization of porcine collateral-dependent coronary arteries. | Contribution of endothelium adaptations to increased KCl-induced contraction cannot be ruled out. | Heaps et al., 2020 |
| | Treadmill running 3–5 mph 5 days/week×14 weeks | HF | Ameroid constrictor | Enhances $K^+$ channel activation. | Inherent variability in collateral development after total occlusion may contribute to variability in experimental responses. | Johnson et al., 2023 |
| | Treadmill running 2–5 mph×14 weeks | HF | Ameroid constrictor | Increases superoxide and NOX4. | Did not identify source of superoxide. | Sytha et al., 2023 |
| | Treadmill running 3–5 mph 5 days/week×8 weeks | HF | Balloon constrictor | Increases VEGF and Flk-1. | Association between exercise intensity and coronary collateral formation remains controversial. | Lu et al., 2008 |
| **ESWT** | 0.09 mJ/mm$^2$, 200 shots/spot×9 spots 3 times in the first week. | HF | Ameroid constrictor | Improves myocardial dysfunction. | Effect of SW on signal transduction after receptor-ligand interaction remains to be clarified. | Nishida et al., 2004 |
| | 0.09 mJ/mm$^2$, 200 shots/spot×27 spots | MI | Coronary artery ligation | Improves LV remodeling. | Whether SW therapy is more effective at suppressing LV remodeling after MI when combined with other drugs is unknown. | Uwatoku et al., 2007 |
| | 0.09 mJ/mm$^2$, 200 shots/spot×27 spots | I/R injury | Interventional surgery (balloon) | Improves LV remodeling after I/R injury. | Effects of SW therapy on each myocardial tissue component remain to be clarified. | Ito et al., 2010 |

Continued

| Rehabilitation treatment | Treatment prescription | Model | | Finding | Limitation | Reference |
|---|---|---|---|---|---|---|
| | 0.09 mJ/mm$^2$, 200 shots/spot×9 or 27 spots 3 times in the first week | MI | Interventional surgery (balloon) | Induces angiogenesis, up-regulates angiogenesis factor expression, and improves reconstruction of microvascular circulation. | Sample size of treatment group is small. | Tao et al., 2011 |
| | 0.09 mJ/mm$^2$, 200 shots/spot×9 spots 3 times in the first week | MI | Interventional surgery (balloon) | Improves myocardial fibrosis by reducing number of fibroblasts. | Whether SW therapy inhibits myocardial fibrosis in infarcted myocardium remains to be examined. | Lei et al., 2013 |
| Low-intensity pulsed ultrasound therapy | Frequency: 1.875 MHz Pulse repetition frequency: 7.10 kHz Cycles: 1, 16, 32, 48, and 64 Strength: 151–193 mW/cm$^2$×3 times | HF | Ameroid constrictor | Cardiac function is significantly improved in LIPUS group. | Optimal number of therapies unclear. | Hanawa et al., 2014 |
| Laser therapy | Ho:YAG laser: 2 J/pulse×10 pulses×6 weeks $CO_2$ laser: 20 J/pulse×6 weeks | HF | Ameroid constrictor | Improves ischemic myocardial function. | Histological findings not explored. | Estvold et al., 2010 |
| | Ga-Al-As diode laser: 1 J/cm$^2$×100 s | MI | Interventional surgery (balloon) | Improves cardiac function. | Number of animals used is not known; Further mechanistic exploration is lacking. | Blatt et al., 2016 |

ESWT: Extracorporeal shock wave therapy; HF: Heart failure; I/R: Ischemia-reperfusion; LV: Left ventricle; MI: Myocardial infarction; mph: Miles per hour; SW: Shock wave.

cardioprotective effects of exercise, elucidating the underlying mechanisms of cardiovascular improvement and establishing a scientific basis for the development of more effective rehabilitation strategies (Figure 4B). Moreover, as clinical IHD patients often require multiple medications, it is essential to understand how exercise influences drug pharmacodynamics and pharmacokinetics, prompting studies in animal models to evaluate these interactions and guide safer, more effective medication use during rehabilitation.

Experimental studies in MI pigs have revealed extensive cardiovascular benefits of exercise training. Exercise reinstates adenosine-induced relaxation and enhances basal tension regulation in distal coronary arterioles, particularly in patients with chronic distal coronary artery occlusion (Heaps et al., 2006, 2000b). Previous studies have shown that pigs exhibit LV dysfunction and neurohumoral activation within the first several weeks after infarction, both of which are modulated by exercise (Haitsma et al., 2001). Long-term exercise enhances myocardial function and improves coronary collateral reserve of the collateral-dependent myocardium (Roth et al., 1990). Exercise also restores the dynamic balance between myocardial oxygen supply and consumption during stress, mediated by enhanced $K_{ATP}^+$- channel-dependent coronary vasodilation (Merkus et al., 2005). Furthermore, impaired $H_2O_2$-mediated vasodilation in porcine collateral-dependent vessels can be rescued through exercise-induced augmentation of $K^+$ channel activity (Johnson et al., 2023).

Exercise also induces coronary vasodilation via multiple vasodilators, including nitric oxide and endothelium-derived hyperpolarization factors (Griffin et al., 1999, 2001; Haitsma et al., 2002). It also modulates redox signaling pathways by promoting the up-regulation of coronary PDE5, superoxide production, and NOX4 activity, thereby refining endothelium-dependent vasodilation of porcine coronary arteries (Sytha et al., 2023; Zheng et al., 2015). Notably, exercise reverses the down-regulation of HSP70 and antioxidant enzymes observed in porcine skeletal muscle following chronic coronary artery occlusion (Lawler et al., 2006) and stimulates coronary collateral formation by up-regulating the expression of angiogenic factors such as VEGF and Flk-1 (Lu et al., 2008).

Beyond vascular adaptations, exercise training modulates cardiac function and pathological remodeling in porcine models of MI. Both exercise and coronary artery occlusion independently promote myocardial hypertrophy and distinct gene expression patterns (Boluyt et al., 2007). Autonomic dysfunction is a common consequence of MI in pigs, characterized by marked suppression of parasympathetic activity, with exercise shown to increase sympathetic drive and reduce myocardial and coronary β-adrenergic reactivity (Duncker et al., 2005). Additionally, Boontje et al. (2011) demonstrated that the preservation of myofilament reactivity following MI is dependent on sustained cMyBP-C phosphorylation, mediated by increased CaMKII-δC activity, which supports the maintenance of diastolic performance during exercise (Boontje et al., 2011).

Understanding how exercise affects the metabolism and distribution of drugs is critical for clinical rehabilitation. For example, in MI pigs, Nω-nitro-L-arginine enhances the vasodilatory action of tezosentan during exercise, while prostaglandins inhibit endothelin-induced coronary vasoconstriction post-MI (de Beer et al., 2011). Cardiomyocyte fibrin sensitization to $Ca^{2+}$ enhances myocardial function during exercise training (Sarin et al., 2011). Furthermore, the positive inotropic effect of the $Ca^{2+}$ sensitizer EMD 57033 is preserved in exercised MI pigs, whereas the efficacy of the $Ca^{2+}$ sensitizer/phosphodiester III inhibitor pimobendan is diminished (Duncker et al., 2001). In addition, $Ca^{2+}$ sensitization enhances the contractile response of collateral-dependent coronary arteries to KCl (Heaps et al., 2020),

highlighting the therapeutic potential of calcium modulators in the context of exercise rehabilitation. Furthermore, Haitsma et al. (2002) reported that agonist-induced vasodilation is weakened early after MI, but exercise maintains endothelial nitric oxide synthase-mediated regulation of vascular tone.

**Exercise protocol::** In most rehabilitation studies, exercise training protocols were structured around sessions performed 5 days per week, typically over a period of 8 to 16 weeks. Each session ranged from 30 to 60 min, with exercise intensity progressively adjusted based on individual animal tolerance to ensure a tailored training regimen. Variations in running speed and session duration accommodated differences in cardiovascular fitness among animals, allowing for gradual workload progression. Protocols were generally divided into four stages: warm-up, sprint, endurance run, and cool-down. The warm-up stage lasted approximately 5 min at an intensity of 2–3 mph (miles per hour). The sprint stage involved running at 5–6 mph for 10–20 min. The endurance stage consisted of running at 2–5 mph for 30–60 min. The session concluded with a cool-down stage, mirroring the warm-up stage at 2–3 mph for an additional 5 min. Some studies also used heart rate as a measure of exercise intensity. For instance, Roth et al. (1990) employed target heart rates of 210–220 beats per minute in their protocol, describing a typical session as follows: “A 5-minute warm-up at 3 km/hr on a 5% incline, followed by 25–45 minutes of running at the target heart rate of 210–220 beats/min. Heart rates were monitored daily via electrocardiogram” (Roth et al., 1990). In this protocol, the treadmill incline was maintained at 0% throughout the study. Animals in the exercise group participated in a progressive treadmill running program for several weeks, while those in the sedentary group remained inactive, confined to their cages during the same period (Heaps et al., 2000a; Muller et al., 1994; Oltman et al., 1995; Parker et al., 1994).

**Extracorporeal shock wave therapy (ESWT)::** Cardiac shock wave therapy has emerged as a promising non-invasive technology for the treatment of cardiovascular diseases, particularly IHD (Myojo et al., 2017; Shkolnik et al., 2018). Cardiac shock wave therapy, sharing fundamental principles of ESWT, harnesses mechanical energy to stimulate tissue repair and regeneration. When applied during reperfusion following MI, ESWT provides immediate cardioprotection, markedly attenuating acute I/R injury and significantly improving LVEF (Petrusca et al., 2023). Initially developed for musculoskeletal and urological applications in rehabilitation medicine, ESWT has demonstrated notable efficacy in cardiac contexts as well (Table 2).The therapeutic effects of ESWT are mediated through multiple biological pathways, including inhibition of cardiomyocyte apoptosis, attenuation of myocardial inflammation, improvement in myocardial fibrosis, reduction of mitochondrial damage and oxidative stress, regulation of cardiomyocyte autophagy, and promotion of endothelial cell angiogenesis, collectively ameliorating myocardial ischemia (Figure 4C).

Preclinical studies using porcine models have provided strong evidence supporting the cardiac benefits of ESWT. Nishida et al. (2004) reported that ESWT significantly improved myocardial dysfunction in a porcine heart failure model induced by coronary ameroid constriction. Subsequent investigations confirmed that ESWT can effectively treat LV remodeling after acute MI caused by thoracotomy ligation (Uwatoku et al., 2007). In acute porcine MI models established by interventional occlusion of the coronary artery, ESWT induced angiogenesis, up-regulated angiogenic factor expression, improved microvascular circulation reconstruction in ischemic myocardia, and reduced myocardial fibrosis by decreasing the number of fibrocytes (Lei et al., 2013; Tao et al., 2011).

Most protocols have employed low-energy ESW, utilizing an energy flux density of 0.09 mJ/mm²—approximately 10% that used in lithotripsy—and delivering 200 shocks per spot across 27 treatment spots. Therapy was typically administered three times during the first week following model establishment (Ito et al., 2010; Lei et al., 2013; Nishida et al., 2004; Tao et al., 2011; Uwatoku et al., 2007). Collectively, these findings underscore the potential of ESWT as a viable therapeutic approach for promoting myocardial repair and mitigating ischemic injury in pigs, offering a strong foundation for clinical translation

**Other physical therapy modalities::** Low-intensity pulsed ultrasound therapy has also emerged as a novel and non-invasive approach for the treatment of IHD. Hanawa et al. (2014) established a porcine HF model via ameroid coarctation and reported that low-intensity pulsed ultrasound therapy normalized myocardial function, increased capillary density in ischemic areas, and increased VEGF, eNOS, and bFGF protein levels in myocardial ischemia. In addition, laser therapy has been reported to improve myocardial function in ischemic territories, while epicardial shock wave therapy has been associated with significant improvements in global ventricular performance in porcine IHD models (Blatt et al., 2016; Estvold et al., 2010; Holfeld et al., 2016). Collectively, these findings provide a robust preclinical foundation supporting the clinical translation of emerging physical therapy modalities for the management of IHD (Table 2).

## DEVELOPMENT OF NEW TECHNIQUES BASED ON PORCINE IHD MODELS

The rapid development of novel technologies, such as gene therapy, cell-based therapy, and nanomaterials, has significantly expanded the application scope of porcine IHD models, providing new avenues for the functional myocardial recovery and precision treatment of cardiovascular conditions. Future therapeutic paradigms are expected to integrate these innovative approaches with various rehabilitation protocols to establish comprehensive, multimodal strategies for IHD management. On this basis, recent progress in the development and clinical application of porcine IHD models is summarized below.

### Development of new techniques based on porcine AS models

In recent years, porcine AS models have served as pivotal platforms for exploring experimental therapeutics, including novel pharmaceuticals, nanotechnology-based interventions, gene therapies, and cytokine-targeted treatments (Table 3). In terms of pharmacological development, porcine AS models have enabled the screening and validation of candidate compounds for their potential therapeutic effects on atherosclerosis and plaque formation and stabilization in the human pathological environment. For instance, corilagin has been reported to reduce vascular injury, lipid plaques, and foam cells (Tao et al., 2021). In addition, these models can facilitate the assessment of commonly used clinical drugs to expand potential indications. Notably, long-term application of vitamin D has been found to improve AS (Rai & Agrawal,

**Table 3 New techniques based on porcine AS models**

| Technique | | Treatment prescription | Model (AS) | Finding | Limitation | Reference |
|---|---|---|---|---|---|---|
| Nanomaterial | anti-LDL SLN | – | High-fat diet | Prevents binding of LDL to scavenger receptors on macrophages present in plaques. | Distribution of SLN *in vivo* is unclear. | du Toit et al., 2022 |
| | SWNT-SHP1i nanotherapy | 400 nmol/L | LDLR-KO+High-fat diet | Reduces vascular inflammation. | Late-stage randomized studies are needed to confirm efficacy. | Bamezai et al., 2024 |
| Gene therapy | ASGR1 KO | – | High-fat diet | Lowers non-HDL-C levels; Fewer atherosclerotic lesions. | Targeted therapy is needed in future exploration. | Xie et al., 2021 |
| Cytokine therapy | IGF-1 | 50 μg/kg s.c. Q12 h×6 months | High-fat diet | Reduces coronary plaque burden and promotes plaque stability. | Small sample size; Safety of treatment needs to be further explored. | Sukhanov et al., 2023 |
| Drug therapy | Pemafibrate (K-877) | 1 mg/kg p.o. QD×8 weeks | LDLR-KO+Balloon compression+High-fat diet | Inhibits inflammatory responses. | Small sample sizes; Differences in other fibrates not compared. | Konishi et al., 2020 |
| | Vitamin D | 1 500 or 3 000 IU/D p.o. QD×6 months | Balloon compression+High-fat diet | Reduces inflammation, neointimal formation, and restenosis. | Small sample sizes; Acute disease conditions not simulated. | Rai & Agrawal, 2021 |
| | Corilagin | 1 mL/kg i.p. QD×12 weeks | Balloon compression+High-fat diet | Reduces degree of vascular injury and number of lipid plaques and foam cells. | Relationship between plaque stability and acute cardiovascular events such as acute coronary syndrome needs to be explored. | Tao et al., 2021 |
| | Atorvastatin | 20 mg p.o. QD×3 months+40 mg p.o. QD×3 months | High-fat diet | Diet quality modulates response of colonic mucosa to atorvastatin treatment but is not associated with development of AS. | High sampling heterogeneity may have resulted in contamination of RNA from neurons and myocytes. | Ye et al., 2021 |
| | GXNT | 162 mg/kg p.o. QD×12 weeks | High-fat diet | Improves CAS. | Specific mechanism of action needs to be further studied. | Yang et al., 2022a |
| | FTZ | 1.2 g/kg p.o. QD×22 weeks | Balloon compression+High-fat diet | Improves CAS by regulating inflammation, reducing apoptosis, and inhibiting EndMT. | Active ingredient of the drug has not been identified. | Wang et al., 2022 |

SLN: Solid lipid nanoparticle; AS: Atherosclerosis; CAS: Coronary atherosclerosis; EndMT: Endothelial to mesenchymal transition; FTZ: Fufang-Zhenzhu-Tiaozhi capsule; GXNT: Guanxinning tablet; LDL: Low-density lipoprotein; SHP1i: Inhibitor of SHP-1; SWNT: Single-walled carbon nanotubes. –: Not available.

2021). Furthermore, various bioactive components derived from traditional Chinese medicine (TCM) have also been developed, demonstrating promising anti-atherosclerotic effects and translational potential (Wang et al., 2022; Yang et al., 2022a).

Gene therapy has also become a powerful tool for elucidating the genetic underpinnings of AS and developing targeted interventions. Porcine models offer a high-fidelity platform for studying specific genes involved in the development of atherosclerosis and for developing gene-specific therapies. Notably, Xie et al. (2021) reported that knockout of ASGR1 significantly reduced atherosclerotic lesion formation, underscoring the potential of genome-editing strategies for disease modification. The application of nanotechnology represents another major frontier. Advanced nanocarrier systems designed for targeted drug delivery and controlled release have demonstrated the potential to enhance therapeutic efficacy while minimizing systemic toxicity (Bamezai et al., 2024; du Toit et al., 2022). The development of these new technologies based on porcine AS models not only promotes cardiovascular disease treatment but also patient recovery.

**Development of new techniques based on porcine MI and I/R injury models**

The advancement of porcine MI and I/R injury models has led to significant progress in IHD research, especially in reducing myocardial injury and improving cardiac function (Tables 4, 5). First, nanomaterials have rapidly emerged as powerful tools in the management of myocardial injury. In porcine I/R injury models, nanoparticles (NPs) and nanofibers have demonstrated substantial potential by enabling the targeted delivery of therapeutic agents directly to ischemic myocardial tissue. Their small size, high surface area, and tunable surface chemistry facilitate precise drug delivery, minimize off-target effects, and improve therapeutic efficacy (Ramirez-Carracedo et al., 2022). Beyond conventional delivery, combining nanomaterials with physical factors has been shown to improve targeting efficiency (Hong et al., 2025). For instance, Jiang et al. (2023) developed an innovative strategy integrating DDFP@NPs with low-intensity focused ultrasound (LIFU) radiation, achieving efficient coronary thrombolysis and improved outcomes in MI pigs.

Important breakthroughs have also been made in the application of cell therapy, cytokine therapy, extracellular vesicle (EV) therapy, and exosome therapy in porcine MI and I/R injury models. Stem cell transplantation has been shown to exert reparative effects through paracrine signaling and cell differentiation, contributing to myocardial regeneration. Moreover, EVs and exosomes, acting as natural carriers of bioactive molecules such as miRNAs, proteins, and other therapeutic substances, have shown potent cardioprotective effects (Li et al., 2023; Wei et al., 2025). Studies have demonstrated that exosome therapy significantly reduces infarct size and improves cardiac function, providing a strong foundation for clinical translation (Li et al., 2024).

Adjunctive modalities such as pharmacological therapy, therapeutic hypothermia, ischemic preconditioning (IPC), and mechanical circulatory support devices have further enriched the therapeutic landscape. Pharmacological interventions

**Table 4 New techniques based on porcine MI models**

| Technique | | Treatment prescription | Model (MI) | Finding | Limitation | Reference |
|---|---|---|---|---|---|---|
| Nanomaterial | HA rTIMP-3 hydrogel | – | Coronary artery ligation | Reduces infarct size. | Small sample size and long-term efficacy is unknown. | Thorn et al., 2023 |
| | LIFU+DDFP@ NPs | LIFU: Frequency of 1 MHz, power of 6 W, irradiation duration of 20 min, duty cycle of 50% for pulse focused ultrasound mode. | Interventional surgery (autologous blood clots) | Reduces infarct size and improves coronary microcirculation. | Efficacy of targeting other infarctions is unknown. | Jiang et al., 2023 |
| Hydrogel | Hydrogel delivery | – | Coronary artery ligation | Improves cardiac function. | Long-term efficacy is unknown. | Avendaño et al., 2023 |
| | Micro-channeled hydrogel suture | – | Coronary artery ligation | Inhibits inflammation, promotes microvascular remodeling. | Small sample size. | Xue et al., 2024 |
| | Highly ROS-eliminating hydrogel | 100 μL×9 sites i.c. | Coronary artery ligation | Improves cardiac function and reduces infarct size and cardiac fibrosis. | Long-term efficacy is unknown. | Wang et al., 2025 |
| Cardiac patch | artCP | Patches are sutured to ischemic tissue | Coronary artery ligation | Reduces scar formation, promotes angiogenesis, improves cardiac function. | Small sample size and long-term efficacy is unknown. | Huang et al., 2020 |
| | BMV-CSC patch | Epicardial suturing of BMV-CSC | Coronary artery ligation | Improves cardiac function, reduces scar area, increases viable myocardial tissue, promotes neovascularization, and inhibits inflammatory responses. | Fabrication of complex cardiac patches is relatively cumbersome. | Su et al., 2020 |
| | ECM patch | – | Coronary artery ligation | Inhibits ECM-induced foreign body inflammatory reactivity. | Small sample size. | Nummi et al., 2022 |
| | Patches incorporating cardiomyocytes | Patches are attached to heart surface using fibrin glue | Coronary artery ligation | Improves cardiac function and reduces infarct area. | Small sample size and potential for clinical translation needs to be further explored. | Wang et al., 2021a |
| Gene therapy | Adenoviral VEGF-$D^{\Delta N\Delta C}$ gene transfer | 200 μL×10 times i.c. | Interventional surgery (permanent coil) | Induces angiogenesis, increases perfusion, improves cardiac function, and increases growth of functional lymphatic networks. | Further studies are needed to optimize beneficial effects, evaluate long-term safety, and identify patient groups that may benefit from treatment. | Pajula et al., 2022 |
| IPC | RIPostC | 4×5 min lower limb I/R | Interventional surgery (balloon+gel sponge) | Preserves myocardial activity, reduces infarct size, and reduces LV remodeling. | Small sample size and therapeutic mechanism needs to be further explored. | Lu et al., 2022 |
| Cell therapy | hiPSC-CMs+Tb4 | 1 mL i.c. | Coronary artery ligation | Induces angiogenesis, promotes proliferation of cardiomyocytes and endothelial cells, improves LV systolic function, and reduces infarct size. | Safety exploration is a key step in translational application. | Tan et al., 2021 |
| | hUMSCs | $1\times10^8$ cells i.c. | Coronary artery ligation | Improves cardiac function. | Long-term efficacy unknown. | Wang et al., 2021b |
| | Stem cell-derived CCPs | $2\times10^8$ cells i.c. | Interventional surgery (balloon) | LVEF improves significantly at 4 and 12 weeks after transplantation. | Difficult to assess effect of CCPs on regeneration without early cardiac function data. | Yap et al., 2023 |
| EV therapy | MSCs-EVs | 1 000 μg i.v. BID×7 days | Coronary artery ligation | Improves cardiac function and reduces infarct size. | Potential immune response after intravenous administration of xenoexosomes not assessed. | Charles et al., 2020 |
| | Exosome spray based on MSCs | 5 mL | Coronary artery ligation | Improves cardiac function and fibrosis. | Small sample size and lack of appropriate clinical scenarios. | Yao et al., 2021 |
| Drug therapy | Dexamethasone | 0.2 mg/kg/d i.m. QD×7 days | Coronary artery ligation | Inhibits CM cytokinesis and functional recovery. | Specific drugs targeting specific immune cells were not used, with their role in acute inflammation after MI in 2-day-old piglets unknown. | Tao et al., 2020 |
| | OFNS | 10 mg/kg p.o. QD×30 days | Interventional surgery (balloon) | Balances intestinal and systemic immune homeostasis for remote cardioprotection. | Effects in PCI patients unknown. | Jia et al., 2023 |

Continued

| Technique | | Treatment prescription | Model (MI) | Finding | Limitation | Reference |
|---|---|---|---|---|---|---|
| | Sacubitril/ valsartan | 49/51 mg sacubitril/valsartan p.o. BID×30 days | Interventional surgery (permanent coil) | Improves inflammation, reduces scar size, reduces rate of ventricular tachycardia induction. | Lack of pharmacokinetic/pharmacodynamic data for sacubitril/valsartan in porcine models. | Martínez-Falguera et al., 2024 |

artCP: Artificial cardiac patch; BID: Bis in die (Twice daily); BMV: Biomimetic microvessel; CCPs: Committed cardiac progenitors; CSCs: Cardiosphere-derived stromal cells; ECM: Extracellular matrix; EVs: Extracellular vesicles; HA: Hyaluronic acid; hiPSC-CMs: Cardiomyocytes derived from human-induced pluripotent stem cells; hUMSCs: Human umbilical cord mesenchymal stem cells; i.c.: Intramyocardial injection; i.m.: Intramuscular injection; I/R: Ischemia-reperfusion; IPC: Ischemic preconditioning; LIFU: Low-intensity focused ultrasound; LV: Left ventricular; LVEF: Left ventricular ejection fraction; MSCs: Mesenchymal stem cells; MI: Myocardial infarction; OFNS: Oral fullerene nanoscavenger; p.o.: Per os; PCI: Percutaneous coronary intervention; QD: Quaque die (Once daily); RIPostC: Remote ischemic postconditioning; ROS: Reactive oxygen species; rTIMP-3: Recombinant TIMP-3. –: Not available.

**Table 5 New techniques based on porcine I/R injury models**

| Technique | | Treatment prescription | Model (I/R injury) | Finding | Limitation | Reference |
|---|---|---|---|---|---|---|
| Nanomaterial | CHIR+FGF1-NPs | 160 μg CHIR+13.3 μg FGF1 | Coronary artery ligation | Reduces infarct size. | Interaction of nanomaterial with these two chemicals is not clear. | Fan et al., 2020 |
| | LNP–TARID | – | Coronary artery ligation | Improves myocardial fibrosis. | Small sample size and lack of mechanistic exploration. | Zhu et al., 2023a |
| | NAP9 | 0.1 mg/kg | Interventional surgery (balloon) | Inhibits extracellular matrix degradation induced by EMMPRIN. | Small sample size and long-term efficacy unknown. | Ramirez-Carracedo et al., 2022 |
| Cardiac patch | Nitrate-functionalized patch | – | Coronary artery ligation | Produces mitochondrial targeted myocardial protection and enhances cardiac repair. | Further studies are needed to reach a consensus on relationship between NO and cardiomyocyte mitosis and cardiac regeneration. | Zhu et al., 2021 |
| Therapeutic hypothermia | Autologous blood transfusion | 27°C | Coronary artery ligation | Limits reperfusion injury. | High mortality rate during IHD model establishment. | Merrill et al., 2020 |
| | MH-SARP | 30 min | Interventional surgery (balloon) | Preserves myocardial function and cellular integrity and reduces infarct size. | Treatment options are not clinically relevant. | Choy et al., 2020 |
| | MTH | ≤35°C | Interventional surgery (balloon) | Does not increase infarct size or prolong treatment time. | Small sample size and high mortality rate during IHD model establishment. | Shanmugasundaram et al., 2021 |
| | Selective intracoronary hypothermia | 4°C | Interventional surgery (balloon) | Preserves mitochondrial integrity. | Proof-of-concept study only. | El Farissi et al., 2022 |
| | MH | 34.5°C | Interventional surgery (balloon) | Hypothermia increases myocardial protection to reduce infarct size. | Hypothermia often requires sedation, which is different from clinical situations. | Berg et al., 2023 |
| | SICH | 30 min | Interventional surgery (balloon) | Reduces infarct size and improves cardiac function. | Lack of attention to changes in acute phase. | Pei et al., 2024 |
| Mechanical LV support | Impella CP | Activate at maximal support (P8)×180 min | Coronary artery ligation | Reduces MI size and MMP-9 and KIM-1 levels. | Future studies exploring long-term impact of AMI and circulatory support on renal function and other biomarkers of kidney injury are needed. | Qiao et al., 2022 |
| | Impella CP | Full pump support×120 min | Interventional surgery (balloon) | Increases blood perfusion in infarct area. | Whether Impella CP can reduce LV minimum pressure and improve tissue perfusion in early diastole remains unclear. | Sakata et al., 2022 |
| | Impella CP | P8×2 h; Impella flow is reduced every 15 min until P0 | Interventional surgery (balloon) | Gradual reloading may be a better strategy. | Small sample size, focuses on mechanical LV unloading in acute MI, and application scope is limited. Not all clinical scenarios were covered. | Mazurek et al., 2024 |
| | Impella CP | Full pump support×90 min | Interventional surgery (balloon) | Increases infarct coronary flow. | Data from relatively acute late reperfusion period, chronic MI, and coronary modulation with long-term LV support not investigated. | Sakata et al., 2024 |
| | Aortix pump | 25 000 r/min×30 min | Interventional surgery (balloon) | Decreases 28-day infarct size. | Small sample size and effect of pumping and coronary flow not evaluated. | Fudim et al., 2025 |

Continued

| Technique | | Treatment prescription | Model (I/R injury) | Finding | Limitation | Reference |
|---|---|---|---|---|---|---|
| Gene therapy | Silencing of lncRNA RMST | AAV6-RMST-specific shRNA (1 mL, $1\times10^{13}$ vg particles) | Coronary artery ligation | Inhibits myocardial fibrosis and improves cardiac function. | Delivery strategy of AAV6-associated gene therapy needs improvement. | Ma et al., 2023a |
| | Depleting anti-CD8 monoclonal antibody | 15 mg/kg | Interventional surgery (balloon) | CD8+ T lymphocyte depletion is protective in pig model of coronary I/R. | Sex differences may affect efficacy. | Santos-Zas et al., 2021 |
| IPC | IPC | 4×5 min/5 min bilateral hindlimb I/R | Coronary artery ligation | Induce release of cardioprotective triggers but does not reduce infarct size. | Pig strain may influence experimental results. | Lieder et al., 2022 |
| | RIPC | 4×5 min hind limb I/R | Coronary artery ligation | Decreases AMI size. HIF pathway likely involved in mechanism of RIPC. | Therapeutic mechanism needs to be further explored. | Anttila et al., 2023 |
| | IPC | 3×5 min LAD occlusion/10 min reperfusion | Coronary artery ligation | Negative result. | Long-term follow-up data are lacking to assess effects of sex differences on long-term efficacy. | Kleinbongard et al., 2023b |
| | IPC | 3×5 min coronary occlusion/10 min reperfusion | Coronary artery ligation | In *Göttingen* minipigs, IPC reduces infarct size, a protective effect absent in *Ossabaw* minipigs. | Therapeutic mechanism needs to be further explored. | Lieder et al., 2023 |
| | IPC | 3×5 min with low pressure inflations | Interventional surgery (balloon) | Alleviates I/R injury. | Time of myocardial reperfusion tissue changes is shorter in pigs. | Binek et al., 2024 |
| Cell therapy | $CCND2^{OE}$CMs | $3\times10^7$ $CCND2^{OE}$ cells i.c. | Coronary artery ligation | Promotes cardiomyocyte proliferation. | Whether injected doses can be transferred to humans requires further study. | Zhao et al., 2021 |
| | Human Muse cells | $1\times10^7$ cells i.v. | Coronary artery ligation | Muse cell product shows good efficacy and safety in treatment of acute MI in miniature pigs. | Sample size of arrhythmia assessment is small, larger samples are needed for verification. | Yamada et al., 2022 |
| | Human placental membrane | HPAC graft (5 cm×5 cm) sutured to infarct area | Coronary artery ligation | Minimizes ischemic injury, preserves cardiac function, and promotes anti-inflammatory pathways. | Therapeutic mechanism needs to be further explored and clinical effects and precise indications still need to be revealed by comprehensive data matrices. | Skaria et al., 2023 |
| | hESC - hEPs | $5\times10^7$ cells i.c. | Coronary artery ligation | Promotes infarct healing. | Real-time plasma concentrations of immunosuppressive agents not measured. Optimal immunosuppressive dose needs to be determined. | Luo et al., 2023 |
| | CCND2-cardiomyocyte SMRTs | SMRTs coding for cardiomyocyte-specific expression of luciferase or GFP | Coronary artery ligation | Promotes cardiomyocyte proliferation, reduces myocardial infarct size, and improves cardiac function. | Results similarly affected by limitations inherent in any human pre-disease clinical model. | Sun et al., 2023 |
| | $^{KO/OE}$hiPSC-CMs | $25\times10^6$ cells i.c. | Coronary artery ligation | Improves cardiac function and reduce infarct size. | Small sample size and snRNA-seq may have missed significantly different gene expression. | Wei et al., 2025 |
| | HUCMSCs+CsA | $5\times10^7$ cells i.v.+5 mg/kg CsA i.v.gtt. | Interventional surgery (balloon) | Reduces acute I/R injury and promotes myocardial repair. | Pure effects of CsA on myocardial IRI not explored. | Liu et al., 2020 |
| | hESC-CMs | $1\times10^9$ cells intrapericardial injections | Interventional surgery (balloon) | Improves myocardial function, increases myocardial mass, and reduces scar tissue. | Differentiation purity needs to be improved. | Shi et al., 2020 |
| | MSCs | $1\times10^6$ cells/kg i.v.gtt. | Interventional surgery (balloon) | Improves microvascular obstruction. | Whether specific immune cell subsets are involved in immunomodulatory effects of MSCs in porcine myocardial I/R injury models needs further investigation. | Wang et al., 2020b |

Continued

| Technique | | Treatment prescription | Model (I/R injury) | Finding | Limitation | Reference |
|---|---|---|---|---|---|---|
| | hMSCs | $75\times10^7$ cells (Mesenchymal stromal cell delivery via *ex vivo* bioreactor preclinical test system) | Interventional surgery (balloon) | Reduces myocardial injury. | Small sample size and long-term efficacy unknown. | O'Rourke et al., 2021 |
| | $(IGF\text{-}1+HGF)^{OE}$ pCPCs | $20\times10^6$ cells | Interventional surgery (balloon) | No significant functional improvement. | Small sample size. | Prat-Vidal et al., 2021 |
| | Allogeneic CDCs | $50\times10^7$ Cells i.c.+$100\times10^7$ Cells i.c. | Interventional surgery (balloon) | Reduces scar size, improves regional systolic function, and attenuates adverse cardiac remodeling. | Number of injected cells needs to be further studied. | Sousonis et al., 2021 |
| | CDCs | $3\times10^5$ cells/kg i.v. | Interventional surgery (balloon) | Changes structure and electrophysiology of scar. | Small sample size and lack of endocardial electrophysiological data. | Arenal et al., 2022 |
| | Human nMSCs+TCM | $(1\text{-}2)\times10^7$ nMSC+2 mg TCM i.c. | Interventional surgery (balloon) | Reduces infarct size and restores cardiac function. | Long-term efficacy unknown. | Bilewska et al., 2022 |
| | S-MenSCs+IFNγ/TNFα-primed MenSCs (S-MenSCs×) | 9.16 mg S-MenSCs or 9.16 mg S-MenSCs×intrapericardial administration | Interventional surgery (balloon) | No significant functional improvement. | Small sample size. | de Pedro et al., 2022 |
| | CDCs+ cyclosporine | $20\times10^6$ CDCs+2.5 mg/kg cyclosporine i.v. ; and 100 mg cyclosporine p.o. QD * 4 weeks | Interventional surgery (balloon) | Oral cyclosporine pretreatment may be necessary to affect cardiac repair with allogeneic CDCs. | Specific mechanism behind complete disappearance of CDCs remains unclear. | Techiryan et al., 2022 |
| | hUCM-MSC | $5\times10^5$ cells/kg i.v. | Interventional surgery (balloon) | Improves LV systolic function. | Difficult to demonstrate total scar tissue volume. | Raposo et al., 2023 |
| | Human CD16+monocytes (hCD16+Ms) | 10×0.3 mL intramyocardial microinjections | Interventional surgery (balloon) | Reduces scar area, increases neovascularization, myofibroblasts, and IL-6 levels, and decreases pro-fibrotic TGF-β levels. | Cell dosage needs to be further studied. | Ascione et al., 2024 |
| Exosome therapy | $hiPSC\text{-}CMs_{EXO}$ | 7.5 mg i.c. | Coronary artery ligation | Promotes myocardial recovery without increasing frequency of arrhythmogenic complications. | Small sample size and small infarct size of model. | Gao et al., 2020 |
| | SCENT | 3×20–30 min inh. | Interventional surgery (balloon) | Improves cardiac function. | Heart retention of inhaled exosomes is limited, and targeting needs to be enhanced. | Li et al., 2024 |
| EV therapy | $M2_{sEVs}$ | 1.0 mg i.c. | Coronary artery ligation | Rescues myocardial function, improves myocardial repair, and modulates $CCR2^+$ macrophages via miR-181b-5p. | Requirement for autologous sEV source and sufficient exosome yield remain key limitations in upscaling sEV‐based therapies. | Li et al., 2023 |
| | $CDC_{EVs}$ | 9.16 mg i.c. | Interventional surgery (balloon) | Regulates immune cells; Reduces inflammatory response. | Molecular mechanisms involved in M2 polarization remain unclear. | López et al., 2020 |
| | $CPC_{sEVs}$ | $20\times10^{11}$ particles i.c. | Interventional surgery (balloon) | Reduces infarct size. | Small sample size and mechanism of sEV uptake is unknown. | Emmert et al., 2024 |
| Cytokine therapy | IGF-1 MSPs | $5\times10^6$ IGF-1 loaded microspheres i.c. | Interventional surgery (balloon) | Improves cardiac function and limits myocardial fibrosis. | Local and circulating levels of IGF-1 not determined. | Báez-Díaz et al., 2020 |
| | HGF MSPs | $5\times10^6$ HGF-loaded microspheres i.c. | Interventional surgery (balloon) | Does not improve cardiac function, reduce inflammation, or myocardial fibrosis. | Animal model is young and does not fit clinical scenario. | Blanco-Blázquez et al., 2023 |

Continued

| Technique | | Treatment prescription | Model (I/R injury) | Finding | Limitation | Reference |
|---|---|---|---|---|---|---|
| | PDGF-AB | 7×65 μg/kg i.v. | Interventional surgery (balloon) | Reduces scar. | Tissue collected at different time points, which may lead to bias in the results. | Hume et al., 2023 |
| MT | MT | 1 or $10\times10^9$ mitochondria i.c. | Coronary artery ligation | Reduces infarct size and enhances cardiac function. | Long-term efficacy unknown. | Guariento et al., 2020 |
| Drug therapy | SGLT2i | 1 mg/kg i.v. | Coronary artery ligation | SGLT2 inhibitors confer cardio-protection in a very short time frame. | Further studies are needed to explore involvement of other pathways or mechanisms. | Baker et al., 2022 |
| | Melatonin | 4 mg/kg i.v. | Coronary artery ligation | Prevents excessive prolongation of QRS interval and Tpeak-Tend interval. | Small sample size. | Bernikova et al., 2022 |
| | N-acetylcysteine | 150 mg/kg i.v.+10 mg/kg i.v. | Coronary artery ligation | Does not protect against reperfusion arrhythmias. | Small sample size and propofol may affect occurrence of arrhythmia, although specific mechanism needs to be further studied. | Haugsten Hansen et al., 2023 |
| | Diazoxide | 7 mg kg i.v. | Coronary artery ligation | Cardio-protection by diazoxide pretreatment is confirmed in adult pigs with reperfused acute MI. | Aortic/coronary perfusion pressure not measured. | Kleinbongard et al., 2023a |
| | metoprolol | 1 mg/kg i.v. | Coronary artery ligation | Metoprolol is not robust to reduced myocardial infarct size in pigs. | Experimental results lack stability. | Kleinbongard et al., 2023c |
| | Melatonin | 4 mg/kg i.v. | Coronary artery ligation | Prevents development of early ventricular fibrillation. | General anesthesia inevitably limits development of *in vivo* experiments due to its inhibitory effects on sympathetic nervous system. | Tsvetkova et al., 2020 |
| | sDR5-Fc | 8 mg/kg i.v. | Coronary artery ligation | Reduces cardiomyocyte death and inflammation. | Potential therapeutic benefit of sDR5-Fc in humans with MI will require future clinical trials. | Wang et al., 2020c |
| | ML355 | 3 mg/kg i.v. | Coronary artery ligation | Attenuates cardiac injury. | Which catalytic or nonenzymatic mechanism dominates is not known. | Zhang et al., 2021 |
| | Vericiguat | 3 mg/kg i.v. | Coronary artery ligation | Alleviates porcine I/R injury by promoting autophagy, preventing apoptosis, and promoting angiogenesis. | Multiple protective mechanisms of Vericigua not fully explored. | Zhu et al., 2023b |
| | Agrin | 33 μg/kg i.c. | Interventional surgery (balloon) | Reduces myocardial I/R injury and improves cardiac function. | More rigorous studies are needed to investigate full spectrum of molecular mechanisms, dose range, toxicity, and pharmacokinetics of Agrin. | Baehr et al., 2020 |
| | DFP | 50 mg/kg p.o. QD×4 weeks | Interventional surgery (balloon) | Reduces myocardial edema and improves adverse remodeling. | Small sample size, limited pathological staining sites, and sex-related drug responses not assessed. | Behrouzi et al., 2020 |
| | Empagliflozin | 10 mg p.o. QD×2 months | Interventional surgery (balloon) | Enhances myocardial deformation. | Whether empagliflozin has additional benefits in acute MI and increased LV filling pressure is unknown. | Garcia-Ropero et al., 2020 |
| | N-SHH | 25 μg/kg i.v. | Interventional surgery (balloon) | Provides effective protection against I/R injury. | Small sample size. | Ghaleh et al., 2020 |
| | Metoprolol | 0.75 mg/kg i.v. | Interventional surgery (balloon) | Reduces incidence of primary ventricular fibrillation. | Poorer collateral circulation in pig heart may translate to more rapid progression of myocardial injury than in patients, affecting experimental results. | Lobo-Gonzalez et al., 2020 |
| | Statin | 0.5 mg/kg i.v. ST+1 mg/kg p.o. QD×6 weeks | Interventional surgery (balloon) | Limits myocardial injury, improves cardiac function, and reduces remodeling. | Drugs are prepared in the laboratory, induced infarction is smaller, and no adjustment for multiple testing. | Mendieta et al., 2020 |

Continued

| Technique | | Treatment prescription | Model (I/R injury) | Finding | Limitation | Reference |
|---|---|---|---|---|---|---|
| | Bufalin+Lycorine | Bufalin 0.1 or 0.2 mg/kg s.c. QD×14 days+0.05 or 0.1 mg/kg s.c. QD×14 days | Interventional surgery (balloon) | Prevents infarct-related LV remodeling, reduces myocardial fibrosis, and increases CDR1as expression. | Lack of healthy control group. | Mester-Tonczar et al., 2020 |
| | Ivabradine | 0.3 mg/kg i.v. | Interventional surgery (balloon) | Exerts myocardial protection by increasing release of EMMPRIN containing cardiac micro-vesicles. | Small sample size and lack of mechanistic exploration. | Ramirez-Carracedo et al., 2020a |
| | ApTOLL | 0.078 mg/kg i.v. | Interventional surgery (balloon) | Improves cardiac function. | Small sample size and lack of mechanistic exploration. | Ramirez-Carracedo et al., 2020b |
| | DMX-10001 | 60 mg/kg/h i.v.×30 min+17 mg/kg/h i.v.× 23.5 h | Interventional surgery (balloon) | Negative result. | Species differences require adjustment of dose. | te Lintel Hekkert et al., 2021 |
| | PGA-diDHA | 65.4 μg/kg i.v. | Interventional surgery (balloon) | Reduces myocardial edema, reduces ischemic risk zone | Stability of preparation needs to be further improved. | Tejedor et al., 2021 |
| | Silybum marianum | 15 mg/kg p.o. QD×15 days | Interventional surgery (balloon) | Reduces plasma triglyceride levels and regulates lipotoxicity. | Small sample size and lack of mechanistic exploration. | Vilahur et al., 2021 |
| | IZD334 | 1 mg/kg, 3 mg/kg, or 10 mg/kg i.v. QD×7 days | Interventional surgery (balloon) | Negative result. | Drug dosing may need further exploration. | Silvis et al., 2022 |
| | Spirulina | 1 g p.o. BID×10 days | Interventional surgery (balloon) | Limits cardiac damage and improves ventricular contractility. | Future studies should investigate effects of spirulina on normal healthy hearts as well as in clinical scenarios combining metabolic comorbidities and IHD. | Vilahur et al., 2022 |
| | DBPR807 | 3 mg/kg i.v. | Interventional surgery (balloon) | Shows potential as an adjunctive medicine for PCI therapies in acute MI patients. | Exact molecular target or biomarker responsible for IRI remains to be determined. | Yeh et al., 2022 |
| | Colchicine | 0.025 mg/kg p.o. Q12H×30 days | Interventional surgery (balloon) | Reduces myocardial fibrosis | Possible toxic and side effects of colchicine not assessed. | Aimo et al., 2023 |
| | Empagliflozin+BOHB | Empagliflozin 10 mg/d p.o. QD×1 week+BOHB 45 mg/kg/h i.v.gtt.×75 min | Interventional surgery (balloon) | Reduces I/R injury; Improves cardiac function. Perioperative intravenous infusion of BOHB induces myocardial protection. | In BOHB group, peak intravenous concentration was measured, differing from steady-state concentration in empagliflozin group. | Santos-Gallego et al., 2023 |
| | Ketone ester | 550 mg/kg p.o. | Interventional surgery (balloon) | Improves myocardial matrix uptake and utilization, improves myocardial ATP levels, and reduces myocardial inflammation. | Small sample size. Different administration methods may have different effects, which need to be further explored. | Yurista et al., 2023 |
| | Mixture of doxycycline, ML-7, and L-NAME | doxycycline (1 μmol/L), ML-7 (0.5 μmol/L), and L-NAME (2 μmol/L) i.c. | Interventional surgery (balloon) | Regulates pro- and antioxidant balance. | Small sample size and lack of mechanistic exploration; Different administration methods may have different effects, which need to be further explored. | Bil-Lula et al., 2024 |
| | ATTM | 15 mg/kg/h i.v.gtt.×1 h | Interventional surgery (balloon) | Exerts therapeutic effects by modulating selenoprotein activity. | Lack of drug dosage and mechanistic exploration. | Johnson et al., 2024 |
| | Infliximab | 5 mg/kg i.v. | Interventional surgery (balloon) | Regulates inflammation, protects myocardium, and reduces structural damage. | Cardiac troponin I (TnI) levels, measured on third day after MI, do not reflect peak concentrations. Lack of mechanistic exploration. | Livia et al., 2024 |
| | MTP-131+VA-ECMO | MTP-1310.05 mg/kg i.v.gtt.+VA-ECMO 7500rmp | Interventional surgery (balloon) | Cardiolipin is an important therapeutic target for VA-ECMO in treatment of acute MI to reduce infarct size and protect mitochondrial function. | Additional studies may be required to test different doses of MTP-131, various ECMO support times, impact of hyperoxemia, and effect of LV unloading on infarct size and cardiolipin metabolism. | Swain et al., 2024 |

Continued

| Technique | Treatment prescription | Model (I/R injury) | Finding | Limitation | Reference |
|---|---|---|---|---|---|
| AZD3366+ticagrelor | 1 or 3 mg/kg AZD3366 i.v.gtt+ticagrelor 90 mg p.o. BID×42 days | Interventional surgery (balloon) | Enhances cardio-protection compared with ticagrelor alone. | Only explored in healthy uncomplicated pigs and does not fit clinical scenario. | Vilahur et al., 2024 |

AMI: Acute myocardial infarction; ApTOLL: A TLR4 antagonist; ATTM: Ammonium tetrathiomolybdate; BID: Bis in die (Twice daily); BOHB: Beta-hydroxybutyrate concentration; CDCs: Cardiosphere-derived cells; CHIR: Wnt1 agonist/GSK-3β antagonist; CsA: Cyclosporin A; DBPR807: CXCR4 antagonist; DFP: Deferiprone; EVs: Extracellular vesicles; GFP: Green fluorescent protein; hESC-CMs: Human embryonic stem cell-derived cardiomyocytes; hESC-hEPs: Human embryonic stem cell-derived epicardial cells; hiPSC-CMs: Cardiomyocytes derived from human-induced pluripotent stem cells; HPAC: Human placental amnion/chorion; hUCM-MSCs: Human umbilical cord matrix-mesenchymal stromal cells; HUCMSCs: Human umbilical cord mesenchymal stem cells; i.c.: Intramyocardial injection; i.v.: Intravenous injection; i.v.gtt.: Intravenous drip; I/R: Ischemia-reperfusion; Inh: inhalation; IHD: Ischemic heart disease; IPC: Ischemic preconditioning; IZD334: NLRP3-inflammasome inhibitor; LNP: Lipid nanoparticle; MenSCs: Menstrual blood-derived mesenchymal stromal cells; MH: Mild hypothermia; MI: Myocardial infarction; ML355: ALOX12 inhibitor; MSCs: Mesenchymal stem cells; MT: Mitochondrial transplantation; MTH: Mild therapeutic hypothermia; NAP9: Nanoparticles conjugated with AP9; NPs: Nanoparticles; N-SHH: Recombinant SHH protein; p.o.: Per os (Oral administration); PCI: Percutaneous coronary intervention; pCPCs: Porcine cardiac progenitor cells; QD: Quaque die (Once daily); RIPC: Remote ischemic preconditioning; RMST: Rhabdomyosarcoma 2-associated transcript; SARP: Selective coronary venous autoretroperfusion; SCENT: Stem cell-derived exosome nebulization therapy; sDR5-Fc: Soluble DR5-Fc; SGLT2i: Sodium glucose co-transporter 2 inhibitor; SICH: Selective intracoronary hypothermia; SMRTs: specific modified mRNA translation system; TARID: lncRNA-Tcf21 antisense RNA inducing demethylation; TCM: total conditioned medium; VA-ECMO: Venoarterial extracorporeal membrane oxygenation. –: Not available.

targeting key pathways involved in MI and I/R injury, including inflammation and oxidative stress, have yielded promising candidates for clinical application (Jia et al., 2023; Livia et al., 2024). Therapeutic hypothermia, by reducing metabolic demand and attenuating ischemia-induced cellular damage, has been optimized in porcine models for effective timing and duration (Berg et al., 2023; Pei et al., 2024). IPC, involving brief cycles of ischemia and reperfusion prior to sustained ischemia, enhances myocardial tolerance to ischemia, with porcine models providing critical insights into strategy refinement (Binek et al., 2024; Lieder et al., 2023). Moreover, mechanical assist devices, such as the Impella CP, have demonstrated significant benefit in maintaining cardiac output in acute I/R injury models. These devices provide temporary mechanical support when cardiac function is damaged and maintain cardiac output, allowing time for myocardial recovery and definitive therapy (Mazurek et al., 2024; Sakata et al., 2024).

Cutting-edge technologies such as gene therapy and mitochondrial transplantation have also been extensively studied in porcine MI and I/R injury models. For example, the silencing of lncRNA RMST has been shown to inhibit myocardial fibrosis and improve cardiac function (Ma et al., 2023a). Furthermore, mitochondrial transplantation has been found to improve heart function by transferring healthy mitochondria to damaged cells to restore energy metabolism and reduce oxidative stress (Guariento et al., 2020). These pioneering approaches, validated in porcine MI and I/R injury models, not only promote basic research but also provide therapeutic avenues for clinical treatment of IHD. Importantly, integrating these advanced therapeutic strategies with structured rehabilitation therapy offers a multidisciplinary approach to IHD management. Such combinations not only optimize treatment effects during the acute stage but also provide comprehensive long-term rehabilitation support for patients, thereby improving clinical prognosis and quality of life.

**Development of new techniques based on porcine HF models**

Porcine models of HF have become indispensable tools for advancing the development of novel regenerative and interventional therapies, offering critical insights into the pathophysiology of HF and facilitating the translation of emerging treatments into clinical practice (Table 6). Among them, cell sheet technology and cardiac patches represent major breakthroughs in myocardial tissue engineering. Cardiac patches combine biomaterials with therapeutic cells to form implantable constructs capable of repairing damaged myocardium. Beyond providing mechanical support to the weakened ventricular wall, these patches actively promote local tissue regeneration by releasing beneficial factors (Dwyer et al., 2023; Miyagawa et al., 2024). Parallel to this, cell sheet technology avoids the limitations of traditional cell injection methods by transplanting contiguous layers of cardiomyocytes or stem cells directly onto the epicardial surface. In porcine HF models, this approach has demonstrated significant improvements in systolic function and reductions in myocardial scar formation, suggesting potent regenerative effects (Gao et al., 2022). The combination of various techniques can better stabilize treatment effects. For example, Sheu et al. (2024) reported that integrating shock wave therapy, adipose-derived mesenchymal stem cell (ADMSC) transplantation, and cell sheet technology markedly improved heart function and ventricular remodeling in HF pigs. However, the precise timing and optimization of ADMSC-cell sheet therapy require further investigation to maximize therapeutic efficacy.

In addition, adeno-associated virus (AAV)-mediated delivery systems have been used in porcine IHD models. Notably, AAV-based inhibition of the Hippo signaling pathway has been shown to reduce refractory arrhythmias after MI (Zhang et al., 2022). Ablation therapy also plays an important role in the management of arrhythmia-related HF. Porcine HF models have been instrumental in optimizing and validating this clinical treatment. Targeted ablation can effectively eliminate lesions with abnormal electrical activity, thereby restoring normal heart rhythm. Particularly, stereotactic body radiation therapy, an emerging modality utilizing high-precision radiation to ablate arrhythmic substrates, has shown encouraging results in porcine HF models, especially for lesions

**Table 6 New techniques based on porcine HF models**

| Technique | | Treatment prescription | Model (HF) | Finding | Limitation | Reference |
|---|---|---|---|---|---|---|
| Nanomaterial | AlgS-NP | 8 mg AlgS-NP (200 μg HGF+IGF-1) i.c. | Interventional surgery (balloon) | Increases cardiac function and improves myocardial remodeling. | Lack of model control group and pharmacokinetic exploration. | Wu et al., 2023 |
| Hydrogel | HA-based hydrogel | 0.1 mL×9 times i.c. | Interventional surgery (balloon) | Smaller strain improvement within infarct and normal regions. | Small sample size and lack of a control group. | Midgett et al., 2022 |
| | dECM/GP hydrogel | Total 2 mL 4 or 5 sites i.c. | Coronary artery ligation | Promotes cell homing and proliferation, inflammation modulation, tissue remodeling, and functional restoration. | Immunogenicity and latent virus of dECM/GP may limit clinical use. | Kong et al., 2023 |
| Cardiac patch | hiPSC-CMs ECT | ECT containing $1\times10^9$ hiPSC-CMs are transplanted onto the infarcted myocardium. | Ameroid constrictor | hiPSC-CM patch successfully implanted in porcine model of chronic myocardial ischemia without arrhythmia. | Results demonstrate successful implantation but do not validate functionality. | Dwyer et al., 2023 |
| | hiPSC-CMs patches | Patch containing $1\times10^8$ cells are transplanted onto the infarcted myocardium. | Ameroid constrictor | Improves cardiac function and promote angiogenesis. | Further studies are needed to evaluate effects of cellular regenerated myocardial tissue on cardiac function. | Miyagawa et al., 2024 |
| Cell sheets | HUCMSCs sheets | Place onto the ischemic area of LV free wall | Ameroid constrictor | Improves cardiac function and reduces infarct size. | Small sample size. *In vivo* real-time monitoring methods for cardiac function should be added to future evaluations. | Gao et al., 2022 |
| | shock wave-pretreated ADMSCs seeded in the cell-sheet scaffold | SW (0.12 mJ/mm 2 for total 140 shots)-pretreated ADMSCs ($1.0\times10^7$) in CSS | Coronary artery ligation | Improves LV remodeling and LVEF | Optimal time point for ADMSC-CSS treatment not explored | Sheu et al., 2024 |
| Gene therapy | 4F gene therapy | Total $3\times10^9$ TU total/pig heart | Interventional surgery (balloon) | Improves LVEF and reduces scar size. | Mechanism of treatment unknown. | Abouleisa et al., 2022 |
| | AAV-*sav*-shRNA | Not reported | Interventional surgery (balloon) | AAV-*Sav*-shRNA gene therapy may have value in treating refractory post infarct arrhythmias. | Small sample size. | Zhang et al., 2022 |
| Cell therapy | Allogeneic BM MSCs | $2\times10^8$ cells every five weeks i.v.gtt.×1 or 3 times | Interventional surgery (balloon) | Improves LVEF and structure, although repeated infusion is required to produce a robust effect. | Infusion dose needs to be further explored. | Tang et al., 2024 |
| | dnHCN4 hiPSC-CMs | $1\times10^9$ cells i.c. | Interventional surgery (balloon) | Intervention insufficient to overcome risk of graft-related arrhythmias. | Further *in vivo* mechanistic exploration is needed to optimize treatment strategies. | Wulkan et al., 2024 |
| | miR-590-3p-overexpressing hiPSC-CMs | $5.0\times10^7$ cells i.c. | Interventional surgery (balloon) | Improves cardiac function. | Acute phase and long-term effects are unknown. | Zhang et al., 2024 |
| Exosome therapy | $CDC_{EXO}$ | 7.5 mg i.c. | Interventional surgery (balloon) | Reduces scar and improves cardiac function. | Lack of attention to changes in acute phase. | Dawkins et al., 2022 |
| Cytokine therapy | NRG-1β | 0.67 mg/kg or 2 mg/kg i.v. BIW×4 weeks | Interventional surgery (balloon) | NRG-1β-mediated anti-atrophic, anti-cachectic effects may provide additional benefits for this potential heart failure therapy. | Further exploration of its role in cardiovascular diseases required at *in vivo* level. | Galindo et al., 2022 |
| | rhPlGF-2 | 5, 15, or 45 μg/kg i.v. QD×14 days | Interventional surgery (balloon) | Therapeutic neovascularization not induced, and no improvement in cardiac function. | Tissue collection at each critical time point after ischemia not covered. | Wu et al., 2024 |
| Ablation therapy | Proton beam therapy | 30 or 40 Gy each target | Interventional surgery (balloon) | Scar significantly homogenized. | Use of amiodarone during experiment affected results. | Hohmann et al., 2020 |
| | PFA | 2000 V for the FOCAL linear catheter or 1800 V for the BASKET catheter | Interventional surgery (balloon) | PFA allows rapid, safe, and effective ablation of surviving islands of myocardium within and around infarcted LV substrate. | Synergistic effect of lidocaine on lesion size cannot be excluded. | Im et al., 2022 |
| | PFA | Monopolar, biphasic waveform of ± 1.3 to 2.0 kV | Interventional surgery (balloon) | PFA may be advantageous for ablation in ventricular scar. | Small sample size. | Younis et al., 2022 |

Continued

| Technique | Treatment prescription | Model (HF) | Finding | Limitation | Reference |
|---|---|---|---|---|---|
| PFA | Electrocardiogram-gated packets of 25 A of monopolar, biphasic, pulsed fields (WAVE1 waveform) | Interventional surgery (balloon) | Viable cardiomyocytes inside and outside scar can be effectively ablated. | Long-term efficacy unknown. | Sandhu et al., 2023 |
| PFA | 1 000–1 500 V pulses | Interventional surgery (balloon) | Ablated lesions shrank within 24 hours to 7 days and remained stable for up to 6 weeks. | cMRI observation and histological examination not completely synchronized. | Miklavčič et al., 2024 |
| Cardiac SBRT | 25 Gy in a single fraction | Interventional surgery (balloon) | Reduces inducibility of ventricular arrhythmias. | Small sample size. Therapeutic mechanism needs to be further explored. | Kancharla et al., 2024 |

4F: Gene Cdk1/CyclinB1 and Cdk4/CyclinD1 complexes; ADMSCs: Adipocyte-derived mesenchymal stem cells; AlgS-NP: Alginate-sulfate nanoparticles; CDC: Cardiosphere-derived cell; cMRI: Cardiac magnetic resonance imaging; CSS: Cell-sheet scaffold; ECM: Extracellular matrix; ECT: Engineered cardiac tissue; GP: Glycopeptide; HA: Hyaluronic acid; HF: Heart failure; hiPSC-CMs: Cardiomyocytes derived from human-induced pluripotent stem cells; HUCMSCs: Human umbilical cord mesenchymal stem cells; i.c.: Intramyocardial injection; i.v.: Intravenous injection; i.v.gtt.: Intravenous drip; LV: Left ventricular; LVEF: Left ventricular ejection fraction; PFA: Pulsed field ablation; SBRT: Stereotactic body radiation therapy.

inaccessible via conventional catheter approaches (Kancharla et al., 2024).

**Clinical translation of emerging techniques based on porcine IHD models**

Several of the above innovative technologies have already progressed to clinical trials or early clinical applications, yielding encouraging results. In particular, significant advances have been achieved in the field of cardiac regeneration through cell-based therapies. Transplantation of autologous or allogeneic stem cells has demonstrated the potential to markedly improve cardiac function in patients following MI. For instance, Attar et al. (2023) reported that intracoronary transplantation of Wharton's jelly-derived mesenchymal stem cells (WJ-MSCs) between 3 and 7 days post-acute MI led to significant improvement in LVEF, with additional gains observed following a booster dose administered 10 days later. Similarly, in patients with LV dysfunction post-MI, the application of cardiosphere-derived cells (CDCs) has been shown to improve segmental heart function (Ostovaneh et al., 2021). Ablation therapy, long established in the clinical treatment of arrhythmias (Gupta et al., 2024), has also seen important refinements, informed in part by studies in porcine models. In patients with refractory ventricular arrhythmias (VA), stereotactic body radiation therapy has been demonstrated to significantly reduce VA load and cardioverter-defibrillator discharge, while delayed-enhancement magnetic resonance imaging offers a promising modality for monitoring treatment effects (Ho et al., 2021). Porcine IHD models are anticipated to remain indispensable for refining and expanding the clinical applicability of these treatment modalities (Kancharla et al., 2024). The success of emerging clinical applications not only validates the translational relevance of porcine models but also strengthens the foundation for continued innovation in IHD therapy.

In addition, the clinical application of pharmacological interventions is gradually being promoted and tested, although findings have been variable. For example, early administration of melatonin in patients with ST-segment elevation MI has been associated with a significant reduction in infarct size after percutaneous coronary intervention (PCI) (Dominguez-Rodriguez et al., 2017a). In contrast, studies utilizing intravenous and intracoronary melatonin injections have reported no reduction in infarct size and have even suggested potential adverse effects on ventricular remodeling and LVEF evolution (Dominguez-Rodriguez et al., 2017b). These conflicting results highlight the complexities of pharmacodynamic responses in the treatment of MI and underscore the necessity of more in-depth and detailed studies to further explore the efficacy and safety of these drugs. Given the close physiological, anatomical, and pathophysiological similarities between pigs and humans, porcine models provide a critical experimental platform and reference basis for the evaluation of drug efficacy and safety.

## CHALLENGES AND OPPORTUNITIES

Porcine disease models offer great potential for advancing cardiovascular research, ranging from the study of pathogenesis to the development and utilization of rehabilitation strategies and even organ transplantation applications (Pilz et al., 2022). Despite the substantial progress made in using porcine models for preclinical rehabilitation studies, no single model can fully replicate the complex and heterogeneous nature of human IHD, with clinical IHD frequently presenting with diverse symptoms and comorbidities (Raj et al., 2015; Shah et al., 2009), complicating the extrapolation of findings from standardized animal models.

Accurately reproducing the full spectrum of IHD features in nonhuman species remains a major challenge. In porcine AS models, variability in the degree, extent, and location of plaque stenosis undermines model stability and reproducibility (Wang et al., 2020a). High-fat diet protocols, while commonly used to induce AS, require extended periods and suffer from inconsistencies, whereas gene-editing approaches, although more precise, are expensive and technically demanding, further complicating model establishment.

Similarly, the induction of MI exhibits substantial interindividual variability among pig breeds, influenced by surgical techniques and infarct size heterogeneity, which compromises the consistency of experimental outcomes. I/R injury models face additional challenges in precisely controlling the onset, severity, and duration of reperfusion injury (Swain et al., 2024; Wei et al., 2025). Establishing HF models often requires prolonged observation periods to

evaluate the efficacy and safety of the model, thereby increasing both time and financial investment. Moreover, limitations in model evaluation methods persist. Histopathology remains the gold standard for lesion assessment but requires animal sacrifice, precluding longitudinal analyses. Most studies rely solely on hematological and imaging indicators, neglecting the multidimensional evaluation of lesion extent, structure, and stage, an approach that diverges from clinical diagnostic standards.

To address these limitations, researchers should carefully select and optimize IHD models according to the scientific questions posed, while considering rehabilitation objectives, technological compatibility, and laboratory feasibility (Solanes et al., 2022). Thoughtful model selection based on experimental goals, logistical constraints, and cost-efficiency will facilitate more rigorous investigations of rehabilitation strategies and their underlying mechanisms. The use of optimized porcine models will not only generate robust preclinical evidence but also pave the way for individualized rehabilitation protocols tailored to patient-specific profiles. Continuous refinement of evaluation techniques is also critical. Emerging evaluation approaches will enable multidimensional assessments of model fidelity and therapeutic outcomes, thus promoting longitudinal analyses of rehabilitation efficacy and facilitating the clinical translation of novel interventions (Amatruda et al., 2014; Dobrucki & Sinusas, 2005). The application of advanced genetic engineering technologies to create precisely modified porcine IHD models represents a particularly promising direction for future research.Several additional challenges warrant attention. First, current cardiac rehabilitation strategies in large animals remain underdeveloped compared to small animal research, underscoring the need to expand and apply innovative physical therapy modalities in porcine models. Second, large animal experiments require rigorous adherence to ethical standards and animal welfare, ensuring humane treatment and respect for animals involved in IHD rehabilitation research. Simultaneously, strict biosafety measures must be maintained to prevent zoonotic disease transmission during large animal experimentation (Wong et al., 2023). In summary, while considerable challenges remain, ongoing technological advances and methodological innovations are expected to elevate the utility of porcine IHD models, ultimately enabling the development of more accurate and effective rehabilitation treatment strategies for IHD patients.

## CONCLUSIONS

This review presents a comprehensive synthesis of current methodologies for the establishment of porcine IHD models and explores relevant research findings related to various rehabilitation strategies and emerging therapeutic technologies. Porcine IHD models have proven instrumental in generating preclinical evidence supporting the application of rehabilitation interventions, elucidating underlying mechanisms, and informing drug use protocols during the rehabilitation process. To date, most preclinical studies employing these models have focused on exercise training as the principal rehabilitation approach, yielding substantial insights into its therapeutic potential. Additionally, modalities such as ESWT, laser therapy, and low-intensity pulsed ultrasound are showing increasing promise for clinical translation in the treatment of IHD.

Critically, porcine models have also served as vital platforms for the evaluation of novel therapies for IHD, including gene therapy, cell-based therapy, and nanomaterial-mediated interventions. These technologies, which directly target myocardial regeneration and functional recovery through precision medicine strategies, have demonstrated encouraging safety and efficacy profiles in large animal experiments. In-depth study and continuous optimization of large animal models have laid a solid foundation for clinical translation. The integration of these innovative technologies with established rehabilitation modalities offers the potential to create comprehensive, individualized rehabilitation strategies tailored to the specific needs of IHD patients.

## COMPETING INTERESTS

The authors declare that they have no competing interests.

## AUTHORS' CONTRIBUTIONS

Concept, Q.W. and C.Y.F.; Resources, Q.W., C.Y.F., and C.Q.H.; Manuscript preparation, S.Q.W., T.Y.C., and L.W.; Revision and editing, all authors. All authors read and approved the final version of the manuscript.

## REFERENCES


Abouleisa RRE, Salama ABM, Ou QH, et al. 2022. Transient cell cycle induction in cardiomyocytes to treat subacute ischemic heart failure. *Circulation*, **145**(17): 1339–1355.

Adeliño R, Martínez-Falguera D, Curiel C, et al. 2022. Electrophysiological effects of adipose graft transposition procedure (AGTP) on the post-myocardial infarction scar: a multimodal characterization of arrhythmogenic substrate. *Frontiers in Cardiovascular Medicine*, **9**: 983001.

Aimo A, Martinez-Falguera D, Barison A, et al. 2023. Colchicine added to standard therapy further reduces fibrosis in pigs with myocardial infarction. *Journal of Cardiovascular Medicine*, **24**(11): 840–846.

Algoet M, Janssens S, Himmelreich U, et al. 2023. Myocardial ischemia-reperfusion injury and the influence of inflammation. *Trends in Cardiovascular Medicine*, **33**(6): 357–366.

Al-Mashhadi RH, Al-Mashhadi AL, Nasr ZP, et al. 2021. Local pressure drives low-density lipoprotein accumulation and coronary atherosclerosis in hypertensive minipigs. *Journal of the American College of Cardiology*, **77**(5): 575–589.

Al-Mashhadi RH, Sørensen CB, Kragh PM, et al. 2013. Familial hypercholesterolemia and atherosclerosis in cloned minipigs created by DNA transposition of a human *PCSK9* gain-of-function mutant. *Science Translational Medicine*, **5**(166): 166ra1.

Amatruda CM, Bona Casas C, Keller BK, et al. 2014. From histology and imaging data to models for in-stent restenosis. *The International Journal of Artificial Organs*, **37**(10): 786–800.

Anttila T, Herajärvi J, Laaksonen H, et al. 2023. Remote ischemic preconditioning and hypoxia-induced biomarkers in acute myocardial infarction: study on a porcine model. *Scandinavian Cardiovascular Journal*, **57**(1): 2251730.

Arce-Esquivel AA, Kreutzer KV, Rush JW, et al. 2012. Exercise does not attenuate early CAD progression in a pig model. *Medicine and Science in Sports and Exercise*, **44**(1): 27–38.

Arenal Á, Ríos-Muñoz GR, Carta-Bergaz A, et al. 2022. Effects of cardiac stem cell on postinfarction arrhythmogenic substrate. *International Journal of Molecular Sciences*, **23**(24): 16211.

Ascione R, Bruno VD, Johnson T, et al. 2024. Intramyocardial immunomodulation with human $CD16^+$ monocytes to treat myocardial infarction in pig: a blind randomized preclinical trial. *Frontiers in Cardiovascular Medicine*, **11**: 1427023.

Attar A, Farjoud Kouhanjani M, Hessami K, et al. 2023. Effect of once versus twice intracoronary injection of allogeneic-derived mesenchymal

stromal cells after acute myocardial infarction: BOOSTER-TAHA7 randomized clinical trial. *Stem Cell Research & Therapy*, **14**(1): 264.

Avendaño R, Midgett D, Melvinsdottir I, et al. 2023. Improvement in cardiac function and regional LV strain following intramyocardial injection of a theranostic hydrogel early postmyocardial infarction in a porcine model. *Journal of Applied Physiology*, **135**(2): 405–420.

Baehr A, Umansky KB, Bassat E, et al. 2020. Agrin promotes coordinated therapeutic processes leading to improved cardiac repair in pigs. *Circulation*, **142**(9): 868–881.

Báez-Díaz C, Blanco-Blázquez V, Sánchez-Margallo FM, et al. 2020. Microencapsulated Insulin-Like Growth Factor-1 therapy improves cardiac function and reduces fibrosis in a porcine acute myocardial infarction model. *Scientific Reports*, **10**(1): 7166.

Baker HE, Tune JD, Mather KJ, et al. 2022. Acute SGLT-2i treatment improves cardiac efficiency during myocardial ischemia independent of $Na^+/H^+$ exchanger-1. *International Journal of Cardiology*, **363**: 138–148.

Bamezai S, Zhang YP, Kumari M, et al. 2024. Pro-efferocytic nanotherapies reduce vascular inflammation without inducing anemia in a large animal model of atherosclerosis. *Nature Communications*, **15**(1): 8034.

Bauer A, McDonald AD, Donahue JK. 2004. Pathophysiological findings in a model of persistent atrial fibrillation and severe congestive heart failure. *Cardiovascular Research*, **61**(4): 764–770.

Behrouzi B, Weyers JJ, Qi XL, et al. 2020. Action of iron chelator on intramyocardial hemorrhage and cardiac remodeling following acute myocardial infarction. *Basic Research in Cardiology*, **115**(3): 24.

Bender SB, de Beer VJ, Tharp DL, et al. 2016. Severe familial hypercholesterolemia impairs the regulation of coronary blood flow and oxygen supply during exercise. *Basic Research in Cardiology*, **111**(6): 61.

Berg J, Jablonowski R, Nordlund D, et al. 2023. Mild hypothermia attenuates ischaemia/reperfusion injury: insights from serial non-invasive pressure-volume loops. *Cardiovascular Research*, **119**(12): 2230–2243.

Bernikova OG, Tsvetkova AS, Ovechkin AO, et al. 2022. ECG markers of acute melatonin treatment in a porcine model of acute myocardial ischemia. *International Journal of Molecular Sciences*, **23**(19): 11800.

Bilewska A, Abdullah M, Mishra R, et al. 2022. Safety and efficacy of transcoronary transfer of human neonatal stem cells to ischemic myocardium using a novel cell-delivery system (CIRCULATE catheter) in swine model of acute myocardial infarction. *Advances in Interventional Cardiology*, **18**(4): 431–438.

Bil-Lula I, Kuliczkowski W, Krzywonos-Zawadzka A, et al. 2024. Mixture of doxycycline, ML-7 and L-NAME restores the pro- and antioxidant balance during myocardial infarction-in vivo pig model study. *Biomedicines*, **12**(4): 784.

Binek A, Castans C, Jorge I, et al. 2024. Oxidative post-translational protein modifications upon ischemia/reperfusion injury. *Antioxidants*, **13**(1): 106.

Blanco-Blázquez V, Báez-Díaz C, Sánchez-Margallo FM, et al. 2023. Intracoronary administration of microencapsulated HGF in a reperfused myocardial infarction swine model. *Journal of Cardiovascular Development and Disease*, **10**(2): 86.

Blatt A, Elbaz-Greener GA, Tuby H, et al. 2016. Low-level laser therapy to the bone marrow reduces scarring and improves heart function post-acute myocardial infarction in the pig. *Photomedicine and Laser Surgery*, **34**(11): 516–524.

Boluyt MO, Cirrincione GM, Loyd AM, et al. 2007. Effects of gradual coronary artery occlusion and exercise training on gene expression in swine heart. *Molecular and Cellular Biochemistry*, **294**(1-2): 87–96.

Boontje NM, Merkus D, Zaremba R, et al. 2011. Enhanced myofilament responsiveness upon β-adrenergic stimulation in post-infarct remodeled myocardium. *Journal of Molecular and Cellular Cardiology*, **50**(3): 487–499.

Boyne P, Billinger SA, Reisman DS, et al. 2023. Optimal intensity and duration of walking rehabilitation in patients with chronic stroke: a randomized clinical trial. *JAMA Neurology*, **80**(4): 342–351.

Brenner GB, Giricz Z, Garamvölgyi R, et al. 2021. Post-myocardial infarction heart failure in closed-chest coronary occlusion/reperfusion model in Göttingen minipigs and landrace pigs. *Journal of Visualized Experiments*, (170): e61901.

Bunker AK, Laughlin MH. 2010. Influence of exercise and perivascular adipose tissue on coronary artery vasomotor function in a familial hypercholesterolemic porcine atherosclerosis model. *Journal of Applied Physiology*, **108**(3): 490–497.

Buszman PP, Orlik B, Milewski KP, et al. 2019. Local intravascular delivery of low-density-lipoprotein cholesterol corresponds with increased intimal thickening in a healthy porcine coronary model. A prelude to development of a model of atherosclerosis. *Advances in Interventional Cardiology*, **15**(1): 81–90.

Charles CJ, Li RR, Yeung T, et al. 2020. Systemic mesenchymal stem cell-derived exosomes reduce myocardial infarct size: characterization with MRI in a porcine model. *Frontiers in Cardiovascular Medicine*, **7**: 601990.

Chen Y, Shao DB, Zhang FX, et al. 2013. Establishment and evaluation of a swine model of acute myocardial infarction and reperfusion-ventricular fibrillation-cardiac arrest using the interventional technique. *Journal of the Chinese Medical Association*, **76**(9): 491–496.

Choy JS, Berwick ZC, Kalasho BD, et al. 2020. Selective autoretroperfusion provides substantial cardioprotection in swine: incremental improvements with mild hypothermia. *JACC: Basic to Translational Science*, **5**(3): 267–278.

Choy JS, Luo T, Huo YL, et al. 2015. Compensatory enlargement of Ossabaw miniature swine coronary arteries in diffuse atherosclerosis. *IJC Heart & Vasculature*, **6**: 4–11.

Davis BT, Wang XJ, Rohret JA, et al. 2014. Targeted disruption of *LDLR* causes hypercholesterolemia and atherosclerosis in Yucatan miniature pigs. *PLoS One*, **9**(4): e93457.

Dawkins JF, Ehdaie A, Rogers R, et al. 2022. Biological substrate modification suppresses ventricular arrhythmias in a porcine model of chronic ischaemic cardiomyopathy. *European Heart Journal*, **43**(22): 2139–2156.

de Beer VJ, Taverne YJ, Kuster DW, et al. 2011. Prostanoids suppress the coronary vasoconstrictor influence of endothelin after myocardial infarction. *American Journal of Physiology: Heart and Circulatory Physiology*, **301**(3): H1080–H1089.

de Pedro MÁ, Pulido M, Marinaro F, et al. 2022. Intrapericardial administration of secretomes from menstrual blood-derived mesenchymal stromal cells: effects on immune-related genes in a porcine model of myocardial infarction. *Biomedicines*, **10**(5): 1117.

Deer RR, Heaps CL. 2013. Exercise training enhances multiple mechanisms of relaxation in coronary arteries from ischemic hearts. *American Journal of Physiology: Heart and Circulatory Physiology*, **305**(9): H1321–H1331.

Dobrucki LW, Sinusas AJ. 2005. Molecular cardiovascular imaging. *Current Cardiology Reports*, **7**(2): 130–135.

Dominguez-Rodriguez A, Abreu-Gonzalez P, de la Torre-Hernandez JM, et al. 2017a. Usefulness of early treatment with melatonin to reduce infarct size in patients with ST-segment elevation myocardial infarction receiving percutaneous coronary intervention (from the melatonin adjunct in the acute myocardial infarction treated with angioplasty trial). *The American Journal of Cardiology*, **120**(4): 522–526.

Dominguez-Rodriguez A, Abreu-Gonzalez P, de la Torre-Hernandez JM, et al. 2017b. Effect of intravenous and intracoronary melatonin as an adjunct to primary percutaneous coronary intervention for acute ST-elevation myocardial infarction: results of the melatonin adjunct in the acute

myocardial infarction treated with angioplasty trial. *Journal of Pineal Research*, **62**(1): e12374.

du Toit LC, Hulisani Demana P, Essop Choonara Y. 2022. A nano-enabled biotinylated anti-LDL theranostic system to modulate systemic LDL cholesterol. *International Journal of Pharmaceutics*, **628**: 122258.

Duan SY, Xing CY, Zhang B, et al. 2015. Detection and evaluation of renal biomarkers in a swine model of acute myocardial infarction and reperfusion. *International Journal of Clinical and Experimental Pathology*, **8**(7): 8336–8347.

Duncker DJ, Haitsma DB, Liem DA, et al. 2001. Beneficial effects of the $Ca^{2+}$ sensitizer EMD 57033 in exercising pigs with infarction-induced chronic left ventricular dysfunction. *British Journal of Pharmacology*, **134**(3): 553–562.

Duncker DJ, Haitsma DB, Liem DA, et al. 2005. Exercise unmasks autonomic dysfunction in swine with a recent myocardial infarction. *Cardiovascular Research*, **65**(4): 889–896.

Dwyer KD, Kant RJ, Soepriatna AH, et al. 2023. One billion hiPSC-cardiomyocytes: upscaling engineered cardiac tissues to create high cell density therapies for clinical translation in heart regeneration. *Bioengineering*, **10**(5): 587.

Eckhouse SR, Jones JA, Spinale FG. 2013. Gene targeting in ischemic heart disease and failure: translational and clinical studies. *Biochemical Pharmacology*, **85**(1): 1–11.

Edwards JM, Neeb ZP, Alloosh MA, et al. 2010. Exercise training decreases store-operated $Ca^{2+}$ entry associated with metabolic syndrome and coronary atherosclerosis. *Cardiovascular Research*, **85**(3): 631–640.

Einstein R, Abdul-Hussein N. 1995. Animal models of heart failure for pharmacological studies. *Clinical and Experimental Pharmacology and Physiology*, **22**(11): 864–868.

El Farissi M, Buscone S, Bax NAM, et al. 2022. Ultrastructural characteristics of myocardial reperfusion injury and effect of selective intracoronary hypothermia: an observational study in isolated beating porcine hearts. *Therapeutic Hypothermia and Temperature Management*, **12**(2): 129–137.

Elagizi A, Kachur S, Carbone S, et al. 2020. A review of obesity, physical activity, and cardiovascular disease. *Current Obesity Reports*, **9**(4): 571–581.

Emini Veseli B, Perrotta P, De Meyer GRA, et al. 2017. Animal models of atherosclerosis. *European Journal of Pharmacology*, **816**: 3–13.

Emmert MY, Burrello J, Wolint P, et al. 2024. Intracoronary delivery of extracellular vesicles from human cardiac progenitor cells reduces infarct size in porcine acute myocardial infarction. *European Heart Journal*, **45**(9): 728–732.

Estvold SK, Mordini F, Zhou YF, et al. 2010. Does laser type impact myocardial function following transmyocardial laser revascularization?. *Lasers in Surgery and Medicine*, **42**(10): 746–751.

Eun K, Hwang SU, Jeong YW, et al. 2017. SV40 large T antigen disrupts embryogenesis of canine and porcine somatic cell nuclear transfer embryo. *Biological Procedures Online*, **19**: 13.

Falk E. 2006. Pathogenesis of atherosclerosis. *Journal of the American College of Cardiology*, **47**(8 Suppl): C7–C12.

Fan CM, Oduk Y, Zhao M, et al. 2020. Myocardial protection by nanomaterials formulated with CHIR99021 and FGF1. *JCI Insight*, **5**(12): e132796.

Fang B, Ren XY, Wang Y, et al. 2018. Apolipoprotein E deficiency accelerates atherosclerosis development in miniature pigs. *Disease Models & Mechanisms*, **11**(10): dmm036632.

Feliciano RDS, Manchini MT, Atum ALB, et al. 2022. Photobiomodulation therapy's effects on cardiac fibrosis activation after experimental myocardial infarction. *Lasers in Surgery and Medicine*, **54**(6): 883–894.

Feng XJ, Chen WX, Ni XY, et al. 2021. Metformin, macrophage dysfunction and atherosclerosis. *Frontiers in Immunology*, **12**: 682853.

Fogarty JA, Delp MD, Muller-Delp JM, et al. 2009. Neuropilin-1 is essential for enhanced $VEGF_{165}$-mediated vasodilatation in collateral-dependent coronary arterioles of exercise-trained pigs. *Journal of Vascular Research*, **46**(2): 152–161.

Fudim M, Konecny F, Heuring JJ, et al. 2025. Left ventricular unloading using intra-aortic entrainment pumping before reperfusion reduces post-AMI infarct size. *Journal of Cardiac Failure*, **31**(3): 538–548.

Galindo CL, Nguyen VT, Hill B, et al. 2022. Neuregulin (NRG-1β) is pro-myogenic and anti-cachectic in respiratory muscles of post-myocardial infarcted swine. *Biology*, **11**(5): 682.

Gao L, Wang L, Wei YH, et al. 2020. Exosomes secreted by hiPSC-derived cardiac cells improve recovery from myocardial infarction in swine. *Science Translational Medicine*, **12**(561): eaay1318.

Gao S, Jin YQ, Ma JL, et al. 2022. Preclinical study of human umbilical cord mesenchymal stem cell sheets for the recovery of ischemic heart tissue. *Stem Cell Research & Therapy*, **13**(1): 252.

Garcia-Ropero A, Santos-Gallego CG, Vargas-Delgado AP, et al. 2020. Correlation between myocardial strain and adverse remodeling in a non-diabetic model of heart failure following empagliflozin therapy. *Expert Review of Cardiovascular Therapy*, **18**(9): 635–642.

Getz GS, Reardon CA. 2022. Pig and mouse models of hyperlipidemia and atherosclerosis. *Methods in Molecular Biology*, **2419**: 379–411.

Ghaleb B, Thireau J, Cazorla O, et al. 2020. Cardioprotective effect of sonic hedgehog ligand in pig models of ischemia reperfusion. *Theranostics*, **10**(9): 4006–4016.

Gill J. 1991. The pathophysiology and epidemiology of myocardial infarction: a review. *Drugs*, **42**(S2): 1–7.

Griffin KL, Laughlin MH, Parker JL. 1999. Exercise training improves endothelium-mediated vasorelaxation after chronic coronary occlusion. *Journal of Applied Physiology*, **87**(5): 1948–1956.

Griffin KL, Woodman CR, Price EM, et al. 2001. Endothelium-mediated relaxation of porcine collateral-dependent arterioles is improved by exercise training. *Circulation*, **104**(12): 1393–1398.

Grinstead WC, Rodgers GP, Mazur W, et al. 1994. Comparison of three porcine restenosis models: the relative importance of hypercholesterolemia, endothelial abrasion, and stenting. *Coronary Artery Disease*, **5**(5): 425–434.

Guariento A, Blitzer D, Doulamis I, et al. 2020. Preischemic autologous mitochondrial transplantation by intracoronary injection for myocardial protection. *The Journal of Thoracic and Cardiovascular Surgery*, **160**(2): e15–e29.

Gupta A, Sattar Z, Chaaban N, et al. 2024. Stereotactic cardiac radiotherapy for refractory ventricular tachycardia in structural heart disease patients: a systematic review. *EP Europace*, **27**(1): euae305.

Haitsma DB, Bac D, Raja N, et al. 2001. Minimal impairment of myocardial blood flow responses to exercise in the remodeled left ventricle early after myocardial infarction, despite significant hemodynamic and neurohumoral alterations. *Cardiovascular Research*, **52**(3): 417–428.

Haitsma DB, Merkus D, Vermeulen J, et al. 2002. Nitric oxide production is maintained in exercising swine with chronic left ventricular dysfunction. *American Journal of Physiology: Heart and Circulatory Physiology*, **282**(6): H2198–H2209.

Hamamdzic D, Wilensky RL. 2013. Porcine models of accelerated coronary atherosclerosis: role of diabetes mellitus and hypercholesterolemia. *Journal of Diabetes Research*, **2013**: 761415.

Han DZ, Yang JJ, Zhang E, et al. 2020. Analysis of mesenchymal stem cell proteomes *in situ* in the ischemic heart. *Theranostics*, **10**(24): 11324–11338.

Hanawa K, Ito K, Aizawa K, et al. 2014. Low-intensity pulsed ultrasound

induces angiogenesis and ameliorates left ventricular dysfunction in a porcine model of chronic myocardial ischemia. *PLoS One*, **9**(8): e104863.

Haugsten Hansen M, Sadredini M, Hasic A, et al. 2023. Myocardial oxidative stress is increased in early reperfusion, but systemic antioxidative therapy does not prevent ischemia-reperfusion arrhythmias in pigs. *Frontiers in Cardiovascular Medicine*, **10**: 1223496.

Heaps CL, Bowles DK, Sturek M, et al. 2000a. Enhanced L-type $Ca^{2+}$ channel current density in coronary smooth muscle of exercise-trained pigs is compensated to limit myoplasmic free $Ca^{2+}$ accumulation. *The Journal of Physiology*, **528**(3): 435–445.

Heaps CL, Bray JF, Parker JL. 2020. Enhanced KCl-mediated contractility and $Ca^{2+}$ sensitization in porcine collateral-dependent coronary arteries persist after exercise training. *American Journal of Physiology: Heart and Circulatory Physiology*, **319**(4): H915–H926.

Heaps CL, Mattox ML, Kelly KA, et al. 2006. Exercise training increases basal tone in arterioles distal to chronic coronary occlusion. *American Journal of Physiology: Heart and Circulatory Physiology*, **290**(3): H1128–H1135.

Heaps CL, Robles JC, Sarin V, et al. 2014. Exercise training-induced adaptations in mediators of sustained endothelium-dependent coronary artery relaxation in a porcine model of ischemic heart disease. *Microcirculation*, **21**(5): 388–400.

Heaps CL, Sturek M, Price EM, et al. 2001. Sarcoplasmic reticulum $Ca^{2+}$ uptake is impaired in coronary smooth muscle distal to coronary occlusion. *American Journal of Physiology: Heart and Circulatory Physiology*, **281**(1): H223–H231.

Heaps CL, Sturek M, Rapps JA, et al. 2000b. Exercise training restores adenosine-induced relaxation in coronary arteries distal to chronic occlusion. *American Journal of Physiology: Heart and Circulatory Physiology*, **278**(6): H1984–H1992.

Henderson KK, Turk JR, Rush JWE, et al. 2004. Endothelial function in coronary arterioles from pigs with early-stage coronary disease induced by high-fat, high-cholesterol diet: effect of exercise. *Journal of Applied Physiology*, **97**(3): 1159–1168.

Heusch G, Libby P, Gersh B, et al. 2014. Cardiovascular remodelling in coronary artery disease and heart failure. *The Lancet*, **383**(9932): 1933–1943.

Ho LT, Chen JLY, Chan HM, et al. 2021. First Asian population study of stereotactic body radiation therapy for ventricular arrhythmias. *Scientific Reports*, **11**(1): 10360.

Hohmann S, Deisher AJ, Konishi H, et al. 2020. Catheter-free ablation of infarct scar through proton beam therapy: tissue effects in a porcine model. *Heart Rhythm*, **17**(12): 2190–2199.

Holfeld J, Zimpfer D, Albrecht-Schgoer K, et al. 2016. Epicardial shock-wave therapy improves ventricular function in a porcine model of ischaemic heart disease. *Journal of Tissue Engineering and Regenerative Medicine*, **10**(12): 1057–1064.

Hong S, Kim J, Chung G, et al. 2025. Revolutionizing drug delivery: low-intensity pulsed ultrasound (LIPUS)-driven deep penetration into hypoxic tumor microenvironments of cholangiocarcinoma. *Theranostics*, **15**(1): 30–51.

Hou NP, Du XG, Wu S. 2022. Advances in pig models of human diseases. *Animal Models and Experimental Medicine*, **5**(2): 141–152.

Huang K, Ozpinar EW, Su T, et al. 2020. An off-the-shelf artificial cardiac patch improves cardiac repair after myocardial infarction in rats and pigs. *Science Translational Medicine*, **12**(538): eaat9683.

Huang L, Hua Z, Xiao H, et al. 2017. CRISPR/Cas9-mediated ApoE-/- and LDLR-/- double gene knockout in pigs elevates serum LDL-C and TC levels. *Oncotarget*, **8**(23): 37751–37760.

Hume RD, Deshmukh T, Doan T, et al. 2023. PDGF-AB reduces myofibroblast differentiation without increasing proliferation after myocardial infarction. *JACC: Basic to Translational Science*, **8**(6): 658–674.

Im SI, Higuchi S, Lee A, et al. 2022. Pulsed field ablation of left ventricular myocardium in a swine infarct model. *JACC: Clinical Electrophysiology*, **8**(6): 722–731.

Ito Y, Ito K, Shiroto T, et al. 2010. Cardiac shock wave therapy ameliorates left ventricular remodeling after myocardial ischemia-reperfusion injury in pigs *in vivo*. *Coronary Artery Disease*, **21**(5): 304–311.

Jensen RV, Hjortbak MV, Bøtker HE. 2020. Ischemic heart disease: an update. *Seminars in Nuclear Medicine*, **50**(3): 195–207.

Jia H, Chang Y, Song JP. 2024. The pig as an optimal animal model for cardiovascular research. *Lab Animal*, **53**(6): 136–147.

Jia W, Sun JC, Cao XR, et al. 2023. Recovering intestinal redox homeostasis to resolve systemic inflammation for preventing remote myocardial injury by oral fullerenes. *Proceedings of the National Academy of Sciences of the United States of America*, **120**(52): e2311673120.

Jiang N, Wang ZW, Deng Q, et al. 2023. Low-intensity focused ultrasound guided dodecafluoropentane-loaded acoustic phase-change nanoparticles for treatment of porcine coronary microthromboembolism. *International Journal of Cardiology*, **371**: 1–9.

Johnson KA, Jeffery E, Bray JF, et al. 2023. Exercise training rescues impaired $H_2O_2$-mediated vasodilation in porcine collateral-dependent coronary arterioles through enhanced $K^+$ channel activation. *American Journal of Physiology: Heart and Circulatory Physiology*, **324**(5): H637–H653.

Johnson TW, Holt J, Kleyman A, et al. 2024. Development and translation of thiometallate sulfide donors using a porcine model of coronary occlusion and reperfusion. *Redox Biology*, **73**: 103167.

Jones JJ, Dietz NJ, Heaps CL, et al. 2001. Calcium buffering in coronary smooth muscle after chronic occlusion and exercise training. *Cardiovascular Research*, **51**(2): 359–367.

Kamato D, Ilyas I, Xu SW, et al. 2022. Non-mouse models of atherosclerosis: approaches to exploring the translational potential of new therapies. *International Journal of Molecular Sciences*, **23**(21): 12964.

Kancharla K, Olson A, Salavatian S, et al. 2024. Ventricular arrhythmia inducibility in porcine infarct model after stereotactic body radiation therapy. *Heart Rhythm*, **21**(7): 1154–1160.

Kim M, Kim HB, Park DS, et al. 2021. A model of atherosclerosis using nicotine with balloon overdilation in a porcine. *Scientific Reports*, **11**(1): 13695.

Kleinbongard P, Lieder H, Skyschally A, et al. 2023a. Diazoxide is a powerful cardioprotectant but is not feasible in a realistic infarct scenario. *Frontiers in Cardiovascular Medicine*, **10**: 1173462.

Kleinbongard P, Lieder H, Skyschally A, et al. 2023b. No sex-related differences in infarct size, no-reflow, and protection by ischaemic pre-conditioning in Göttingen minipigs. *Cardiovascular Research*, **119**(2): 561–570.

Kleinbongard P, Lieder HR, Skyschally A, et al. 2023c. No robust reduction of infarct size and no-reflow by metoprolol pretreatment in adult Göttingen minipigs. *Basic Research in Cardiology*, **118**(1): 23.

Kong PX, Dong J, Li WC, et al. 2023. Extracellular matrix/glycopeptide hybrid hydrogel as an immunomodulatory niche for endogenous cardiac repair after myocardial infarction. *Advanced Science*, **10**(23): 2301244.

Konishi H, Miyauchi K, Onishi A, et al. 2020. Effect of pemafibrate (K-877), a novel selective peroxisome proliferator-activated receptor α modular (SPPARMα), in atherosclerosis model using low density lipoprotein receptor knock-out swine with balloon injury. *PLoS One*, **15**(11): e0241195.

Korzick DH, Rishel ME, Bowles DK. 2005. Exercise and hypercholesterolemia produce disparate shifts in coronary PKC expression. *Medicine and Science in Sports and Exercise*, **37**(3): 381–388.

Kuwahara M, Tsujino Y, Tsubone H, et al. 2004. Effects of pair housing on

diurnal rhythms of heart rate and heart rate variability in miniature swine. *Experimental Animals*, **53**(4): 303–309.

Lawler JM, Kwak HB, Song W, et al. 2006. Exercise training reverses downregulation of HSP70 and antioxidant enzymes in porcine skeletal muscle after chronic coronary artery occlusion. *American Journal of Physiology: Regulatory, Integrative and Comparative Physiology*, **291**(6): R1756–R1763.

Lee SG, Oh J, Bong SK, et al. 2018. Macrophage polarization and acceleration of atherosclerotic plaques in a swine model. *PLoS One*, **13**(3): e0193005.

Lei PP, Tao SM, Shuai Q, et al. 2013. Extracorporeal cardiac shock wave therapy ameliorates myocardial fibrosis by decreasing the amount of fibrocytes after acute myocardial infarction in pigs. *Coronary Artery Disease*, **24**(6): 509–515.

Li JL, Sun SH, Zhu DS, et al. 2024. Inhalable stem cell exosomes promote heart repair after myocardial infarction. *Circulation*, **150**(9): 710–723.

Li L, Cao JS, Li S, et al. 2023. M2 Macrophage-derived sEV regulate pro-Inflammatory $CCR2^+$ macrophage subpopulations to favor post-AMI cardiac repair. *Advanced Science*, **10**(14): 2202964.

Li X, Tan W, Li X, et al. 2022. A surgical model of heart failure with preserved ejection fraction in *Tibetan* minipigs. *Journal of Visualized Experiments*, (180): e63526.

Li YX, Fuchimoto D, Sudo M, et al. 2016. Development of human-like advanced coronary plaques in low-density lipoprotein receptor knockout pigs and justification for statin treatment before formation of atherosclerotic plaques. *Journal of the American Heart Association*, **5**(4): e002779.

Lian NQ, Tong J, Li WW, et al. 2018. Ginkgetin ameliorates experimental atherosclerosis in rats. *Biomedicine & Pharmacotherapy*, **102**: 510–516.

Liao YT, Li H, Cao H, et al. 2021. Therapeutic silencing miR-146b-5p improves cardiac remodeling in a porcine model of myocardial infarction by modulating the wound reparative phenotype. *Protein & Cell*, **12**(3): 194–212.

Lieder HR, Adam V, Skyschally A, et al. 2023. Attenuation of ST-segment elevation by ischemic preconditioning: reflection of cardioprotection in Göttingen but not in Ossabaw minipigs. *International Journal of Cardiology*, **386**: 109–117.

Lieder HR, Skyschally A, Sturek M, et al. 2022. Remote ischemic conditioning in Ossabaw minipigs induces the release of humoral cardioprotective triggers, but the myocardium does not respond with reduced infarct size. *American Journal of Physiology: Heart and Circulatory Physiology*, **323**(6): H1365–H1375.

Liu C, Kang LN, Chen F, et al. 2020. Immediate intracoronary delivery of human umbilical cord mesenchymal stem cells reduces myocardial injury by regulating the inflammatory process through cell-cell contact with T lymphocytes. *Stem Cells and Development*, **29**(20): 1331–1345.

Livia C, Inglis S, Crespo-Diaz R, et al. 2024. Infliximab limits injury in myocardial infarction. *Journal of the American Heart Association*, **13**(9): e032172.

Lobo-Gonzalez M, Galán-Arriola C, Rossello X, et al. 2020. Metoprolol blunts the time-dependent progression of infarct size. *Basic Research in Cardiology*, **115**(5): 55.

Loen V, Smoczynska A, Aranda Hernandez A, et al. 2023. Automatic measurement of short-term variability of repolarization to indicate ventricular arrhythmias in a porcine model of cardiac ischaemia. *EP Europace*, **25**(11): euad341.

López E, Blázquez R, Marinaro F, et al. 2020. The intrapericardial delivery of extracellular vesicles from cardiosphere-derived cells stimulates M2 polarization during the acute phase of porcine myocardial infarction. *Stem Cell Reviews and Reports*, **16**(3): 612–625.

Lou X, Tang YW, Ye L, et al. 2023. Cardiac muscle patches containing four types of cardiac cells derived from human pluripotent stem cells improve recovery from cardiac injury in mice. *Cardiovascular Research*, **119**(4): 1062–1076.

Lu X, Wu T, Huang P, et al. 2008. Effect and mechanism of intermittent myocardial ischemia induced by exercise on coronary collateral formation. *American Journal of Physical Medicine & Rehabilitation*, **87**(10): 803–814.

Lu Y, Tian Y, Mou TT, et al. 2022. Transient cardioprotective effects of remote ischemic postconditioning on non-reperfused myocardial infarction: longitudinal evaluation study in pigs. *International Journal of Cardiology*, **355**: 37–43.

Lunney JK, Van Goor A, Walker KE, et al. 2021. Importance of the pig as a human biomedical model. *Science Translational Medicine*, **13**(621): eabd5758.

Luo XL, Jiang Y, Li Q, et al. 2023. hESC-derived epicardial cells promote repair of infarcted hearts in mouse and swine. *Advanced Science*, **10**(27): 2300470.

Ma T, Qiu F, Gong YS, et al. 2023a. Therapeutic silencing of lncRNA RMST alleviates cardiac fibrosis and improves heart function after myocardial infarction in mice and swine. *Theranostics*, **13**(11): 3826–3843.

Ma ZH, Mao CF, Chen X, et al. 2023b. Peptide vaccine against ADAMTS-7 ameliorates atherosclerosis and postinjury neointima hyperplasia. *Circulation*, **147**(9): 728–742.

Martínez-Falguera D, Aranyó J, Teis A, et al. 2024. Antiarrhythmic and anti-inflammatory effects of sacubitril/valsartan on post-myocardial infarction scar. *Circulation: Arrhythmia and Electrophysiology*, **17**(5): e012517.

Martínez-Falguera D, Fadeuilhe E, Teis A, et al. 2021. Myocardial infarction by percutaneous embolization coil deployment in a swine model. *Journal of Visualized Experiments*, (177): e63172.

Mazurek R, Kariya T, Sakata T, et al. 2024. Negative impact of acute reloading after mechanical left ventricular unloading. *Journal of Cardiovascular Translational Research*, **17**(2): 233–241.

Mendieta G, Ben-Aicha S, Gutiérrez M, et al. 2020. Intravenous statin administration during myocardial infarction compared with oral post-infarct administration. *Journal of the American College of Cardiology*, **75**(12): 1386–1402.

Merkus D, Houweling B, de Beer VJ, et al. 2007. Alterations in endothelial control of the pulmonary circulation in exercising swine with secondary pulmonary hypertension after myocardial infarction. *The Journal of Physiology*, **580**(3): 907–923.

Merkus D, Houweling B, van Vliet M, et al. 2005. Contribution of $K_{ATP}^+$ channels to coronary vasomotor tone regulation is enhanced in exercising swine with a recent myocardial infarction. *American Journal of Physiology: Heart and Circulatory Physiology*, **288**(3): H1306–H1313.

Merrill TL, Mitchell JE, Merrill DR, et al. 2020. Myocardial tissue salvage is correlated with ischemic border region temperature at reperfusion. *Catheterization and Cardiovascular Interventions*, **96**(6): E593–E601.

Mester-Tonczar J, Winkler J, Einzinger P, et al. 2020. Association between circular RNA CDR1as and post-infarction cardiac function in pig ischemic heart failure: influence of the anti-fibrotic natural compounds bufalin and lycorine. *Biomolecules*, **10**(8): 1180.

Midgett DE, Thorn SL, Ahn SS, et al. 2022. CineCT platform for in vivo and ex vivo measurement of 3D high resolution Lagrangian strains in the left ventricle following myocardial infarction and intramyocardial delivery of theranostic hydrogel. *Journal of Molecular and Cellular Cardiology*, **166**: 74–90.

Miklavčič D, Verma A, Krahn PRP, et al. 2024. Biophysics and electrophysiology of pulsed field ablation in normal and infarcted porcine cardiac ventricular tissue. *Scientific Reports*, **14**(1): 32063.

Miller V, Mente A, Dehghan M, et al. 2017. Fruit, vegetable, and legume intake, and cardiovascular disease and deaths in 18 countries (PURE): a prospective cohort study. *The Lancet*, **390**(10107): 2037–2049.

Miyagawa S, Kawamura T, Ito E, et al. 2024. Pre-clinical evaluation of the

efficacy and safety of human induced pluripotent stem cell-derived cardiomyocyte patch. *Stem Cell Research & Therapy*, **15**(1): 73.

Miyagi C, Miyamoto T, Kuroda T, et al. 2022. Large animal models of heart failure with preserved ejection fraction. *Heart Failure Reviews*, **27**(2): 595–608.

Muller JM, Myers PR, Laughlin MH. 1994. Vasodilator responses of coronary resistance arteries of exercise-trained pigs. *Circulation*, **89**(5): 2308–2314.

Myojo M, Ando J, Uehara M, et al. 2017. Feasibility of extracorporeal shock wave myocardial revascularization therapy for post-acute myocardial infarction patients and refractory angina pectoris patients. *International Heart Journal*, **58**(2): 185–190.

Netzley AH, Pelled G. 2023. The pig as a translational animal model for biobehavioral and neurotrauma research. *Biomedicines*, **11**(8): 2165.

Niccoli G, Scalone G, Lerman A, et al. 2016. Coronary microvascular obstruction in acute myocardial infarction. *European Heart Journal*, **37**(13): 1024–1033.

Nishida T, Shimokawa H, Oi K, et al. 2004. Extracorporeal cardiac shock wave therapy markedly ameliorates ischemia-induced myocardial dysfunction in pigs in vivo. *Circulation*, **110**(19): 3055–3061.

Nummi A, Pätilä T, Mulari S, et al. 2022. Epicardial transplantation of autologous atrial appendage micrografts: evaluation of safety and feasibility in pigs after coronary artery occlusion. *Scandinavian Cardiovascular Journal*, **56**(1): 352–360.

Ogita M, Miyauchi K, Onishi A, et al. 2016. Development of accelerated coronary atherosclerosis model using low density lipoprotein receptor knock-out swine with balloon injury. *PLoS One*, **11**(9): e0163055.

Olivari D, De Giorgio D, Staszewsky LI, et al. 2022. Searching for preclinical models of acute decompensated heart failure: a concise narrative overview and a novel swine model. *Cardiovascular Drugs and Therapy*, **36**(4): 727–738.

Oltman CL, Parker JL, Laughlin MH. 1995. Endothelium-dependent vasodilation of proximal coronary arteries from exercise-trained pigs. *Journal of Applied Physiology*, **79**(1): 33–40.

O'Rourke B, Nguyen S, Tilles AW, et al. 2021. Mesenchymal stromal cell delivery via an ex vivo bioreactor preclinical test system attenuates clot formation for intravascular application. *Stem Cells Translational Medicine*, **10**(6): 883–894.

Ostovaneh MR, Makkar RR, Ambale-Venkatesh B, et al. 2021. Effect of cardiosphere-derived cells on segmental myocardial function after myocardial infarction: ALLSTAR randomised clinical trial. *Open Heart*, **8**(2): e001614

Pagliaro BR, Cannata F, Stefanini GG, et al. 2020. Myocardial ischemia and coronary disease in heart failure. *Heart Failure Reviews*, **25**(1): 53–65.

Pajula J, Lähteenvuo J, Lähteenvuo M, et al. 2022. Adenoviral VEGF-D$^{\Delta N\ \Delta C}$ gene therapy for myocardial ischemia. *Frontiers in Bioengineering and Biotechnology*, **10**: 999226.

Parker JL, Oltman CL, Muller JM, et al. 1994. Effects of exercise training on regulation of tone in coronary arteries and arterioles. *Medicine and Science in Sports and Exercise*, **26**(10): 1252–1261.

Patel N, Johnson MA, Vapniarsky N, et al. 2023. Elamipretide mitigates ischemia-reperfusion injury in a swine model of hemorrhagic shock. *Scientific Reports*, **13**(1): 4496.

Pei ZQ, Qiu J, Zhao YC, et al. 2024. A novel intracoronary hypothermia device reduces myocardial reperfusion injury in pigs. *Chinese Medical Journal*, **137**(20): 2461–2472.

Petrusca L, Croisille P, Augeul L, et al. 2023. Cardioprotective effects of shock wave therapy: a cardiac magnetic resonance imaging study on acute ischemia-reperfusion injury. *Frontiers in Cardiovascular Medicine*, **10**: 1134389.

Pilz PM, Ward JE, Chang WT, et al. 2022. Large and small animal models of heart failure with reduced ejection fraction. *Circulation Research*, **130**(12): 1888–1905.

Poulsen CB, Pedrigi RM, Pareek N, et al. 2018. Plaque burden influences accurate classification of fibrous cap atheroma by in vivo optical coherence tomography in a porcine model of advanced coronary atherosclerosis. *EuroIntervention*, **14**(10): 1129–1135.

Prat-Vidal C, Crisóstomo V, Moscoso I, et al. 2021. Intracoronary delivery of porcine cardiac progenitor cells overexpressing IGF-1 and HGF in a pig model of sub-acute myocardial infarction. *Cells*, **10**(10): 2571.

Qiao XY, Bhave S, Swain L, et al. 2022. Myocardial injury promotes matrix metalloproteinase-9 activity in the renal cortex in preclinical models of acute myocardial infarction. *Journal of Cardiovascular Translational Research*, **15**(2): 207–216.

Qin XH, Cai PA, Liu C, et al. 2023. Cardioprotective effect of ultrasound-targeted destruction of Sirt3-loaded cationic microbubbles in a large animal model of pathological cardiac hypertrophy. *Acta Biomaterialia*, **164**: 604–625.

Rai V, Agrawal DK. 2021. Immunomodulation of IL-33 and IL-37 with vitamin D in the neointima of coronary artery: a comparative study between balloon angioplasty and stent in hyperlipidemic microswine. *International Journal of Molecular Sciences*, **22**(16): 8824.

Raj P, Zieroth S, Netticadan T. 2015. An overview of the efficacy of resveratrol in the management of ischemic heart disease. *Annals of the New York Academy of Sciences*, **1348**(1): 55–67.

Ramirez-Carracedo R, Sanmartin M, Ten A, et al. 2022. Theranostic contribution of extracellular matrix metalloprotease inducer-paramagnetic nanoparticles against acute myocardial infarction in a pig model of coronary ischemia-reperfusion. *Circulation: Cardiovascular Imaging*, **15**(6): e013379.

Ramirez-Carracedo R, Tesoro L, Hernandez I, et al. 2020a. Ivabradine-stimulated microvesicle release induces cardiac protection against acute myocardial infarction. *International Journal of Molecular Sciences*, **21**(18): 6566.

Ramirez-Carracedo R, Tesoro L, Hernandez I, et al. 2020b. Targeting TLR4 with ApTOLL improves heart function in response to coronary ischemia reperfusion in pigs undergoing acute myocardial infarction. *Biomolecules*, **10**(8): 1167.

Raposo L, Cerqueira RJ, Leite S, et al. 2023. Human-umbilical cord matrix mesenchymal cells improved left ventricular contractility independently of infarct size in swine myocardial infarction with reperfusion. *Frontiers in Cardiovascular Medicine*, **10**: 1186574.

Richardson MR, Lai XY, Dixon JL, et al. 2009. Diabetic dyslipidemia and exercise alter the plasma low-density lipoproteome in Yucatan pigs. *Proteomics*, **9**(9): 2468–2483.

Robles JC, Heaps CL. 2015. Adaptations of the endothelin system after exercise training in a porcine model of ischemic heart disease. *Microcirculation*, **22**(1): 68–78.

Roth DM, White FC, Nichols ML, et al. 1990. Effect of long-term exercise on regional myocardial function and coronary collateral development after gradual coronary artery occlusion in pigs. *Circulation*, **82**(5): 1778–1789.

Sakaguchi G, Sakakibara Y, Tambara K, et al. 2003. A pig model of chronic heart failure by intracoronary embolization with gelatin sponge. *The Annals of Thoracic Surgery*, **75**(6): 1942–1947.

Sakata T, Mavropoulos SA, Mazurek R, et al. 2024. Reduction of left ventricular diastolic pressure as a key regulator of infarct coronary flow under mechanical left ventricular support. *The Journal of Physiology*, **602**(8): 1669–1680.

Sakata T, Watanabe S, Mazurek R, et al. 2022. Impaired diastolic function predicts improved ischemic myocardial flow by mechanical left ventricular unloading in a swine model of ischemic heart failure. *Frontiers in Cardiovascular Medicine*, **8**: 795322.

Sandhu U, Alkukhun L, Kheiri B, et al. 2023. *In vivo* pulsed-field ablation in

healthy vs. chronically infarcted ventricular myocardium: biophysical and histologic characterization. *EP Europace*, **25**(4): 1503–1509.

Santos-Gallego CG, Requena-Ibáñez JA, Picatoste B, et al. 2023. Cardioprotective effect of empagliflozin and circulating ketone bodies during acute myocardial infarction. *Circulation: Cardiovascular Imaging*, **16**(4): e015298.

Santos-Zas I, Lemarié J, Zlatanova I, et al. 2021. Cytotoxic $CD8^+$ T cells promote granzyme B-dependent adverse post-ischemic cardiac remodeling. *Nature Communications*, **12**(1): 1483.

Sarin V, Muthuchamy M, Heaps CL. 2011. $Ca^{2+}$ sensitization of cardiac myofilament proteins contributes to exercise training-enhanced myocardial function in a porcine model of chronic occlusion. *American Journal of Physiology: Heart and Circulatory Physiology*, **301**(4): H1579–H1587.

Schüttler D, Tomsits P, Bleyer C, et al. 2022. A practical guide to setting up pig models for cardiovascular catheterization, electrophysiological assessment and heart disease research. *Lab Animal*, **51**(2): 46–67.

Shah DJ, Kim HW, Kim RJ. 2009. Evaluation of ischemic heart disease. *Heart Failure Clinics*, **5**(3): 315–332.

Shanmugasundaram M, Truong HT, Harhash A, et al. 2021. Extending time to reperfusion with mild therapeutic hypothermia: a new paradigm for providing primary percutaneous coronary intervention to remote ST segment elevation myocardial infarction patients. *Therapeutic Hypothermia and Temperature Management*, **11**(1): 45–52.

Sheu JJ, Yeh JN, Chen YC, et al. 2024. Shock wave-pretreated ADMSCs of cell-sheet scaffold (CSS) patched on the left ventricular wall (LVW) inhibited LVW remodeling in mini-pig MI: role of CSS on counteracting Laplace's Law of LVW stress - experimental study. *International Journal of Surgery*, **110**(12): 7546–7562.

Shi YJ, Zhao Y, Li Y, et al. 2020. High concentrations of H7 human embryonic stem cells at the point of care for acute myocardial infarction. *Annals of Translational Medicine*, **8**(22): 1510.

Shim J, Al-Mashhadi RH, Sørensen CB, et al. 2016. Large animal models of atherosclerosis-new tools for persistent problems in cardiovascular medicine. *The Journal of Pathology*, **238**(2): 257–266.

Shim J, Poulsen CB, Hagensen MK, et al. 2017. Apolipoprotein E deficiency increases remnant lipoproteins and accelerates progressive atherosclerosis, but not xanthoma formation, in gene-modified minipigs. *JACC: Basic to Translational Science*, **2**(5): 591–600.

Shkolnik E, Burneikaite G, Celutkiene J, et al. 2018. Efficacy of cardiac shock wave therapy in patients with stable angina: the design of randomized, triple blind, sham-procedure controlled study. *Anatolian Journal of Cardiology*, **19**(2): 100–109.

Silvis MJM, Demkes EJ, Timmers L, et al. 2022. NLRP3-inflammasome inhibition with IZD334 does not reduce cardiac damage in a pig model of myocardial infarction. *Biomedicines*, **10**(12): 3056.

Simmons GH, Padilla J, Jenkins NT, et al. 2014. Exercise training and vascular cell phenotype in a swine model of familial hypercholesterolaemia: conduit arteries and veins. *Experimental Physiology*, **99**(2): 454–465.

Simon F, Larena-Avellaneda A, Wipper S. 2022. Experimental atherosclerosis research on large and small animal models in vascular surgery. *Journal of Vascular Research*, **59**(4): 221–228.

Skaria RS, Lopez-Pier MA, Kathuria BS, et al. 2023. Epicardial placement of human placental membrane protects from heart injury in a swine model of myocardial infarction. *Physiological Reports*, **11**(20): e15838.

Solanes N, Bobi J, Arrieta M, et al. 2022. An open secret in porcine acute myocardial infarction models: the relevance of anaesthetic regime and breed in ischaemic outcomes. *Frontiers in Veterinary Science*, **9**: 919454.

Sousonis V, Sfakianaki T, Ntalianis A, et al. 2021. Intracoronary administration of allogeneic cardiosphere-derived cells immediately prior to reperfusion in pigs with acute myocardial infarction reduces infarct size and attenuates adverse cardiac remodeling. *Journal of Cardiovascular Pharmacology and Therapeutics*, **26**(1): 88–99.

Stevic N, Pinède A, Mewton N, et al. 2024. Effect of ventricular fibrillation on infarct size after myocardial infarction: a translational study. *Basic Research in Cardiology*, **119**(6): 911–921.

Su T, Huang K, Mathews KG, et al. 2020. Cardiac stromal cell patch integrated with engineered microvessels improves recovery from myocardial infarction in rats and pigs. *ACS Biomaterials Science & Engineering*, **6**(11): 6309–6320.

Sukhanov S, Higashi Y, Yoshida T, et al. 2023. Insulin-like growth factor 1 reduces coronary atherosclerosis in pigs with familial hypercholesterolemia. *JCI Insight*, **8**(4): e165713.

Sun JC, Wang L, Matthews RC, et al. 2023. CCND2 modified mRNA activates cell cycle of cardiomyocytes in hearts with myocardial infarction in mice and pigs. *Circulation Research*, **133**(6): 484–504.

Sun K, Han RJ, Zhao RP, et al. 2018. Evaluation of dual energy computed tomography iodine mapping within the myocardial blood pool for detection of acute myocardial infarction: correlation with histopathological findings in a porcine model. *The British Journal of Radiology*, **91**(1087): 20170569.

Sun SJ, Jiang Y, Zhen Z, et al. 2020. Establishing a swine model of post-myocardial infarction heart failure for stem cell treatment. *Journal of Visualized Experiments*, (159): e60392.

Swain L, Bhave S, Qiao XY, et al. 2024. Novel role for cardiolipin as a target of therapy to mitigate myocardial injury caused by venoarterial extracorporeal membrane oxygenation. *Circulation*, **149**(17): 1341–1353.

Sytha SP, Bray JF, Heaps CL. 2023. Exercise induces superoxide and NOX4 contribution in endothelium-dependent dilation in coronary arterioles from a swine model of chronic myocardial ischemia. *Microvascular Research*, **150**: 104590.

Tan SH, Loo SJ, Gao Y, et al. 2021. Thymosin β4 increases cardiac cell proliferation, cell engraftment, and the reparative potency of human induced-pluripotent stem cell-derived cardiomyocytes in a porcine model of acute myocardial infarction. *Theranostics*, **11**(16): 7879–7895.

Tang XL, Wysoczynski M, Gumpert AM, et al. 2024. Intravenous infusions of mesenchymal stromal cells have cumulative beneficial effects in a porcine model of chronic ischaemic cardiomyopathy. *Cardiovascular Research*, **120**(15): 1939–1952.

Tao SM, Guo T, Wang Y, et al. 2011. Extracorporeal cardiac shock wave therapy improved myocardial micro-vascular circulation after acute myocardial infarction at early stage in pigs. *Journal of Sichuan University (Medical Science Edition)*, **42**(2): 222–226. (in Chinese)

Tao YT, Zhang L, Yang RH, et al. 2021. Corilagin ameliorates atherosclerosis by regulating MMP-1, -2, and -9 expression *in vitro* and *in vivo*. *European Journal of Pharmacology*, **906**: 174200.

Tao ZH, Loo S, Su LP, et al. 2020. Dexamethasone inhibits regeneration and causes ventricular aneurysm in the neonatal porcine heart after myocardial infarction. *Journal of Molecular and Cellular Cardiology*, **144**: 15–23.

te Lintel Hekkert M, Newton G, Chapman K, et al. 2021. Preclinical trial of a MAP4K4 inhibitor to reduce infarct size in the pig: does cardioprotection in human stem cell-derived myocytes predict success in large mammals?. *Basic Research in Cardiology*, **116**(1): 34.

Techiryan G, Weil BR, Young RF, et al. 2022. Widespread intracoronary allogeneic cardiosphere-derived cell therapy with and without cyclosporine in reperfused myocardial infarction. *American Journal of Physiology: Heart and Circulatory Physiology*, **323**(5): H904–H916.

Tejedor S, Dolz-Pérez I, Decker CG, et al. 2021. Polymer conjugation of docosahexaenoic acid potentiates cardioprotective therapy in preclinical models of myocardial ischemia/reperfusion injury. *Advanced Healthcare Materials*, **10**(9): 2002121.

Tharp DL, Masseau I, Ivey J, et al. 2019. Endurance exercise training does not limit coronary atherosclerosis in familial hypercholesterolemic swine.

*Physiological Reports*, **7**(4): e14008.
Thengchaisri N, Shipley R, Ren Y, et al. 2007. Exercise training restores coronary arteriolar dilation to NOS activation distal to coronary artery occlusion: role of hydrogen peroxide. *Arteriosclerosis, Thrombosis, and Vascular Biology*, **27**(4): 791–798.
Thirugnanasambandam M, Frey S, Rösch Y, et al. 2022. Effect of collateral flow on catheter-based assessment of cardiac microvascular obstruction. *Annals of Biomedical Engineering*, **50**(9): 1090–1102.
Thorn SL, Shuman JA, Stacy MR, et al. 2023. Matrix metalloproteinase-targeted SPECT/CT imaging for evaluation of therapeutic hydrogels for the early modulation of post-infarct myocardial remodeling. *Journal of Cardiovascular Translational Research*, **16**(1): 155–165.
Tsvetkova AS, Bernikova OG, Mikhaleva NJ, et al. 2020. Melatonin prevents early but not delayed ventricular fibrillation in the experimental porcine model of acute ischemia. *International Journal of Molecular Sciences*, **22**(1): 328.
Uwatoku T, Ito K, Abe K, et al. 2007. Extracorporeal cardiac shock wave therapy improves left ventricular remodeling after acute myocardial infarction in pigs. *Coronary Artery Disease*, **18**(5): 397–404.
Vilahur G, Radike M, Sutelman P, et al. 2024. Recombinant human soluble domain of CD39L3 and ticagrelor: cardioprotective effects in experimental myocardial infarction. *European Heart Journal*, **45**(17): 1553–1567.
Vilahur G, Sutelman P, Ben-Aicha S, et al. 2022. Supplementation with spirulina reduces infarct size and ameliorates cardiac function in a pig model of STEMI. *Frontiers in Pharmacology*, **13**: 891801.
Vilahur G, Sutelman P, Mendieta G, et al. 2021. Triglyceride-induced cardiac lipotoxicity is mitigated by *Silybum marianum*. *Atherosclerosis*, **324**: 91–101.
Völz S, Redfors B, Angerås O, et al. 2021. Long-term mortality in patients with ischaemic heart failure revascularized with coronary artery bypass grafting or percutaneous coronary intervention: insights from the Swedish Coronary Angiography and Angioplasty Registry (SCAAR). *European Heart Journal*, **42**(27): 2657–2664.
Wang DY, Xu XQ, Zhao MJ, et al. 2020a. Accelerated miniature swine models of advanced atherosclerosis: a review based on morphology. *Cardiovascular Pathology*, **49**: 107241.
Wang JZ, Chen ZW, Dai Q, et al. 2020b. Intravenously delivered mesenchymal stem cells prevent microvascular obstruction formation after myocardial ischemia/reperfusion injury. *Basic Research in Cardiology*, **115**(4): 40.
Wang K, Wen J, Liang T, et al. 2025. Enhancing miR-19a/b induced cardiomyocyte proliferation in infarcted hearts by alleviating oxidant stress and controlling miR-19 release. *Biomaterials*, **312**: 122732.
Wang LX, Zhang DX, Zhan WJ, et al. 2022. Chinese medicine Fufang Zhenzhu Tiaozhi capsule ameliorates coronary atherosclerosis in diabetes mellitus-related coronary heart disease minipigs. *Biomedicine & Pharmacotherapy*, **156**: 113831.
Wang LY, Liu YQ, Ye GL, et al. 2021a. Injectable and conductive cardiac patches repair infarcted myocardium in rats and minipigs. *Nature Biomedical Engineering*, **5**(10): 1157–1173.
Wang Q, He XJ, Wang B, et al. 2021b. Injectable collagen scaffold promotes swine myocardial infarction recovery by long-term local retention of transplanted human umbilical cord mesenchymal stem cells. *Science China Life Sciences*, **64**(2): 269–281.
Wang Y, Chen L, Wang L, et al. 2023. Pulsed electromagnetic fields combined with adipose-derived stem cells protect ischemic myocardium by regulating miR-20a-5p/E2F1/p73 signaling. *Stem Cells*, **41**(7): 724–737.
Wang YH, Zhang HL, Wang ZZ, et al. 2020c. Blocking the death checkpoint protein TRAIL improves cardiac function after myocardial infarction in monkeys, pigs, and rats. *Science Translational Medicine*, **12**(540): eaaw3172.
Wei YH, Walcott G, Nguyen T, et al. 2025. Follistatin from hiPSC-cardiomyocytes promotes myocyte proliferation in pigs with postinfarction LV remodeling. *Circulation Research*, **136**(2): 161–176.
Wong ML, Zulzahrin Z, Vythilingam I, et al. 2023. Perspectives of vector management in the control and elimination of vector-borne zoonoses. *Frontiers in Microbiology*, **14**: 1135977.
Wu M, Pelacho B, Claus P, et al. 2023. Alginate sulfate-nanoparticles loaded with hepatocyte growth factor and insulin-like growth factor-1 improve left ventricular repair in a porcine model of myocardial ischemia reperfusion injury. *European Journal of Pharmaceutics and Biopharmaceutics*, **184**: 83–91.
Wu M, Pokreisz P, Claus P, et al. 2024. Recombinant human placental growth factor-2 in post-infarction left ventricular dysfunction: a randomized, placebo-controlled, preclinical study. *Basic Research in Cardiology*, **119**(5): 795–806.
Wulkan F, Romagnuolo R, Qiang BP, et al. 2024. Stem cell-derived cardiomyocytes expressing a dominant negative pacemaker HCN4 channel do not reduce the risk of graft-related arrhythmias. *Frontiers in Cardiovascular Medicine*, **11**: 1374881.
Xie BC, Shi XC, Li Y, et al. 2021. Deficiency of ASGR1 in pigs recapitulates reduced risk factor for cardiovascular disease in humans. *PLoS Genetics*, **17**(11): e1009891.
Xie W, Parker JL, Heaps CL. 2012. Effect of exercise training on nitric oxide and superoxide/$H_2O_2$ signaling pathways in collateral-dependent porcine coronary arterioles. *Journal of Applied Physiology*, **112**(9): 1546–1555.
Xin W, Li XY, Lu XY, et al. 2011. Involvement of endoplasmic reticulum stress-associated apoptosis in a heart failure model induced by chronic myocardial ischemia. *International Journal of Molecular Medicine*, **27**(4): 503–509.
Xue FC, Zhao SL, Tian H, et al. 2024. Two way workable microchanneled hydrogel suture to diagnose, treat and monitor the infarcted heart. *Nature Communications*, **15**(1): 864.
Yamada Y, Minatoguchi S, Baba S, et al. 2022. Human Muse cells reduce myocardial infarct size and improve cardiac function without causing arrythmias in a swine model of acute myocardial infarction. *PLoS One*, **17**(3): e0265347.
Yang FH, Pyle WG, Bei YH. 2023. Innovative animal models of cardiac remodeling: development and evaluation. *Journal of Visualized Experiments*, (193): e65019.
Yang QQ, Xu YY, Shen LY, et al. 2022a. Guanxinning tablet attenuates coronary atherosclerosis via regulating the gut microbiota and their metabolites in Tibetan minipigs induced by a high-fat diet. *Journal of Immunology Research*, **2022**: 7128230.
Yang SP, Ma JT, Li T, et al. 2022b. Radioiodinated hypericin as a tracer for detection of acute myocardial infarction: SPECT-CT imaging in a swine model. *Journal of Nuclear Cardiology*, **29**(6): 3432–3439.
Yang Y, Jones AW, Thomas TR, et al. 2007. Influence of sex, high-fat diet, and exercise training on potassium currents of swine coronary smooth muscle. *American Journal of Physiology: Heart and Circulatory Physiology*, **293**(3): H1553–H1563.
Yao JL, Huang K, Zhu DS, et al. 2021. A minimally invasive exosome spray repairs heart after myocardial infarction. *ACS Nano*, **15**(7): 11099–11111.
Yap L, Chong LY, Tan C, et al. 2023. Pluripotent stem cell-derived committed cardiac progenitors remuscularize damaged ischemic hearts and improve their function in pigs. *npj Regenerative Medicine*, **8**(1): 26.
Ye SM, Matthan NR, Lamon-Fava S, et al. 2021. Colon transcriptome is modified by a dietary pattern/atorvastatin interaction in the Ossabaw pig. *The Journal of Nutritional Biochemistry*, **90**: 108570.
Yeh KC, Lee CJ, Song JS, et al. 2022. Protective effect of CXCR4 antagonist DBPR807 against ischemia-reperfusion injury in a rat and porcine model of myocardial infarction: potential adjunctive therapy for

percutaneous coronary intervention. *International Journal of Molecular Sciences*, **23**(19): 11730.

Younis A, Zilberman I, Krywanczyk A, et al. 2022. Effect of pulsed-field and radiofrequency ablation on heterogeneous ventricular scar in a swine model of healed myocardial infarction. *Circulation: Arrhythmia and Electrophysiology*, **15**(10): e011209.

Yuan F, Guo L, Park KH, et al. 2018. Ossabaw pigs with a PCSK9 gain-of-function mutation develop accelerated coronary atherosclerotic lesions: a novel model for preclinical studies. *Journal of the American Heart Association*, **7**(6): e006207.

Yurista SR, Eder RA, Welsh A, et al. 2023. Ketone ester supplementation suppresses cardiac inflammation and improves cardiac energetics in a swine model of acute myocardial infarction. *Metabolism: Clinical and Experimental*, **145**: 155608.

Zhang S, Liu SJ, Leach JP, et al. 2022. Gene therapy knockdown of hippo signaling resolves arrhythmic events in pigs after myocardial infarction. *Circulation*, **146**(20): 1558–1560.

Zhang XJ, Liu XL, Hu ML, et al. 2021. Pharmacological inhibition of arachidonate 12-lipoxygenase ameliorates myocardial ischemia-reperfusion injury in multiple species. *Cell Metabolism*, **33**(10): 2059–2075. e10.

Zhang ZW, Li XT, Zhuang JW, et al. 2024. miR-590–3p overexpression improves the efficacy of hiPSC-CMs for myocardial repair. *JACC: Basic to Translational Science*, **9**(5): 557–573.

Zhao M, Nakada Y, Wei YH, et al. 2021. Cyclin D2 overexpression enhances the efficacy of human induced pluripotent stem cell-derived cardiomyocytes for myocardial repair in a swine model of myocardial infarction. *Circulation*, **144**(3): 210–228.

Zheng XX, Heaps CL, Fisher SA. 2015. Myosin phosphatase isoforms and related transcripts in the pig coronary circulation and effects of exercise and chronic occlusion. *Microvascular Research*, **98**: 166–171.

Zhou LH, Sun JT, Yang TT, et al. 2023. Improved methodology for efficient establishment of the myocardial ischemia-reperfusion model in pigs through the median thoracic incision. *Journal of Biomedical Research*, **37**(4): 315–325.

Zhou ML, Widmer RJ, Xie W, et al. 2010. Effects of exercise training on cellular mechanisms of endothelial nitric oxide synthase regulation in coronary arteries after chronic occlusion. *American Journal of Physiology: Heart and Circulatory Physiology*, **298**(6): H1857–H1869.

Zhu DS, Hou JL, Qian M, et al. 2021. Nitrate-functionalized patch confers cardioprotection and improves heart repair after myocardial infarction via local nitric oxide delivery. *Nature Communications*, **12**(1): 4501.

Zhu DS, Liu S, Huang K, et al. 2023a. Intrapericardial long non-coding RNA-*Tcf21* antisense RNA inducing demethylation administration promotes cardiac repair. *European Heart Journal*, **44**(19): 1748–1760.

Zhu WD, Ben Y, Shen Y, et al. 2023b. Vericiguat protects against cardiac damage in a pig model of ischemia/reperfusion. *PLoS One*, **18**(12): e0295566.

Zwack CC, Haghani M, Hollings M, et al. 2023. The evolution of digital health technologies in cardiovascular disease research. *npj Digital Medicine*, **6**(1): 1.